CAPITAL UNIVERSITY OF SCIENCE AND TECHNOLOGY, ISLAMABAD

Acoustic Wave Scattering from Membrane Panels in Waveguides with Plane Wave and Piston Radiations

by

Muhammad Ismaeel

A thesis submitted in partial fulfillment for the degree of Master of Philosophy

in the

Faculty of Computing
Department of Mathematics

2024

I dedicate this effort to my Family, my dear Parents, my elegant Teachers and my supervisor Dr. Muhammad Afzal who are always source of inspiration for me and their contributions are uncounted.

CERTIFICATE OF APPROVAL

Acoustic Wave Scattering from Membrane Panels in Waveguides with Plane Wave and Piston Radiations

by

Muhammad Ismaeel

(MMT213007)

THESIS EXAMINING COMMITTEE

(a)	External Examiner	Dr. Amer Bilal Mann	FUUAST, Islamabad
(b)	Internal Examiner	Dr. Abdul Rehman Kashif	CUST, Islamabad
(c)	Supervisor	Dr. Muhammad Afzal	CUST, Islamabad

Dr. Muhammad Afzal
Thesis Supervisor
October, 2024

Dr. Muhammad Sagheer
Head
Dept. of Mathematics
October, 2024

Dr. Muhammad Abdul Qadir
Dean
Faculty of Computing
October, 2024

Author's Declaration

I, **Muhammad Ismaeel**, hereby state that my MPhil thesis titled "**Acoustic Wave Scattering from Membrane Panels in Waveguides with Plane Wave and Piston Radiations**" is my work and has not been submitted previously by me for taking any degree from Capital University of Science and Technology, Islamabad or anywhere else in the country/abroad.

At any time if my statement is found to be incorrect even after my graduation, the University has the right to withdraw my MPhil Degree.

(Muhammad Ismaeel)

Registration No: MMT213007

Plagiarism Undertaking

I solemnly declare that the research work presented in this thesis is titled "**Acoustic Wave Scattering from Membrane Panels in Waveguides with Plane Wave and Piston Radiations**" is solely my research work with no significant contribution from any other person. Small contribution/help wherever taken has been dully acknowledged and that complete thesis has been written by me.

I understand the zero tolerance policy of the HEC and Capital University of Science and Technology towards plagiarism. Therefore, I as an author of the above-titled thesis declare that no portion of my thesis has been plagiarized and any material used as reference is properly referred/cited.

I undertake that if I am found guilty of any formal plagiarism in the above-titled thesis even after awarded of MPhil Degree, the University reserves the right to withdraw/revoke my MPhil degree and that HEC and the University have the right to publish my name on the HEC/University website on which names of students are placed who submitted plagiarized work.

(Muhammad Ismaeel)

Registration No: MMT213007

Acknowledgement

I got no words to articulate my cordial sense of gratitude to **Almighty Allah** who is the most merciful and most beneficent to his creation.

I also express my gratitude to the last prophet of **Almighty Allah, Prophet Muhammad (PBUH)** the supreme reformer of the world and knowledge for a human being.

I would like to be thankful to all those who provided support and encouraged me during this work.

I would like to be grateful to my thesis supervisor **Dr. Muhammad Afzal**, for guiding and encouraging me in writing this thesis. It would have remained incomplete without his endeavours. Due to his efforts, I was able to write and complete this assertation.

I would like to pay great tribute to my **parents**, for their prayers, moral support, encouragement and appreciation.

Last but not the least, I want to express my gratitude to my **friends** who helped me throughout my MPhil degree.

(Muhammad Ismaeel)

Abstract

The current thesis is focused on modeling and analyzing the scattering of planar waves and piston radiations emitted from membrane panels. These membranes are situated within cylindrical waveguides and are connected to the surface using spring-like conditions. The physical modeling of wave propagation leads to a set of differential equations, including Helmholtz's equation with the membrane equation, rigid conditions, and impedance conditions. The mode matching method is utilized to solve the governing boundary value problems. To enforce the edge conditions, the Dirac delta function is employed. Eigenfunction expansion with unknown amplitudes is discovered in duct regions, and matching conditions at the interfaces aid in converting the differential system into a linear algebraic system, which is then truncated and solved. The truncated solution satisfies the matching conditions and conserves the law of energy.

Contents

List of Figures

Abbreviations

BVP	Boundary value problem
HVAC	Heating, Ventilation, and Air Conditioning
MM	Mode-matching
WH	Wiener-Hopf

Symbols

c	Speed of sound
C_p	Constant pressure
C_v	Constant volume
k	Wave number
u	Flow velocity
τ	Stress tensor
α	Transverse wavenumber
g	Gravitational acceleration
p	Instantaneous pressure
p_0	Equilibrium pressure
T	Temperature
ω	Frequency
ρ	Instantaneous density
ρ_0	Equilibrium density
r	Specific gas constant
ρg	Body forces
∇	Divergence
∇_p	Exerting force
γ	Ratio of specific heat
β	Bulk modulus
ϕ	Fluid velocity potential
$\hat{Z}$	Impedance
a	Dimensional radius
η_n,δ_{mn}	Axial wavenumber , Kronecker delta

Chapter 1

Introduction

The most significant environmental issue of our time is noise pollution, which not only interferes with our daily lives but also poses a significant threat to human health and well-being. Exposure to noise has a multifaceted impact on human health, manifesting in physiological effects, such as elevated blood pressure and headaches , psychological effects, including stress and anxiety and social consequences, leading to feelings of isolation and segregation. Main noise sources include traffic, planes, trains, construction, and industry. To reduce noise, control measures like silencers are used in vehicle exhausts, featuring geometric designs and sound-absorbing materials that minimize engine and fan vibrations, effectively reducing noise levels.

Noise pollution is a significant concern in contemporary society, encompassing both outdoor and indoor sources of noise. Among the primary contributors to noise pollution are the exhaust systems of vehicles, aircraft, power plants, and heating, ventilation, and air conditioning (HVAC) units. Addressing noise and its associated vibrations necessitates the investigation and design of structures that transmit noise. Many exhaust systems are equipped with silencers, typically comprising perforated sections that allow emissions to dissipate within a chamber before exiting the system. While these waveguides often feature rectangular cross-sections, circular configurations are also common. Therefore, the examination of acoustic scattering in circular cylindrical shells remains a subject of ongoing interest in engineering and applied mathematics, particularly regarding the impact of

discontinuities on wave propagation. The most basic circular cylindrical structure involves a rigid wall that neither supports vibrations nor absorbs acoustic waves. The current work is related theoretical study of elastic membrane with microperforated holes. The mode matching technique is adopted to analyze the scattering behavior of incoming propagative modes in the presence of membrane. The propagation of modes is linked with the eigenvalues and eigenvectors of transformed system. To ensure the accuracy of collected modes two simple duct problems are considered. First problem is bounded by rigid walls and is excited with a plane piston along the wall whereas, in the later problem the upper horizontal wall is replaced with impedance surface. Both of these problems are solved with mod matching technique. To analyze performance of physical system the model coefficients are ploted for different velocities of moving piston. The aforementioned worked is comprehensively discussed in Chapter 3. Wherease the effects of locally reacting liners in the cavities of the chamber are discussed in Chapter 4.

1.1 Literature Review

Sound waves, a fundamental aspect of human experience, have been present since the dawn of humanity. In the 6th century BC, the Greek philosopher Pythagoras laid the foundations for the scientific study of acoustics. Through his innovative experiments, he discovered the relationship between string tension and pitch, and explored the tones produced by striking objects. Building upon this legacy, we continue to investigate the propagation and scattering of acoustic waves at interfaces, including the effects of membranes and rigid boundaries. Our inquiry is a testament to the enduring power of Pythagoras' insights, which have inspired generations of scholars and scientists to explore the harmony of the universe. Later, Galileo discovered the correlation between a string's pitch and its vibrating length. Building on this foundation, Joseph Sauveur explored the relationship between frequency and pitch, while Marin Mersenne successfully determined the frequency associated with a given pitch. These groundbreaking discoveries laid the groundwork

for our understanding of acoustics and sound waves. In the 19th century, Wheatstone, Ohm, and Henry recognized a fundamental analogy between electricity and acoustics, laying the groundwork for future advancements. The 20th century witnessed significant technological innovations in acoustic systems. Notably, Sabine's pioneering work in architectural acoustics led to the development of submarine detection technologies, marking a significant milestone in the application of acoustic principles. This breakthrough paved the way for further innovations in acoustic engineering and its diverse applications. This thesis investigates acoustic scattering phenomena in cylindrical waveguides, specifically focusing on the behavior of micro-perforated membranes in these structures. The research explores the complex interactions between sound waves and the perforated membrane, aiming to enhance our understanding of acoustic scattering and its applications in various fields.

Shenderove [54] modeled that the sound field in a waveguide as the superposition of normal waves, whose mode shapes are deduced by the separation of variable technique. He postulated that a propagation in the positive direction can be expressed as the combination of function that are partial solutions to the Helmholt'z equation. Kirby [25] considered two different silencers of an exhaust system radiated from inlet pipe. He equiped the device with reactive and dissiptive tools and concluded that the acoustic behavior of energy in silencers can be improved for higher frequency modes by reactive and dissipative materials. Denia et al. [16] demonstrated that in the automotive exhaust system, dissipative silencers have been shown to providedesirable noise control. Because broad band sound attenuation occurs in the mid and high frequency ranges. Abom's[1] research explored the design of an expansion chamber with extended inlet and outlet ducts, forming a concentric duct structure. The study investigated the acoustic performance of this device, taking into account the effects of uniform and reactive linings at both ends of the chamber. The dispersion of waves through different layered media is discussed in [21, 36, 42–45]. Research on dissipative expansion chambers has been extensive. Cummings and Chang [15] utilized a mode-matching technique to determine the transmission loss of such a chamber, including the impact of mean flow. Xu et al.[62] developed a 2D analytical solution, employing a pressure and

velocity matching technique, to examine the acoustic performance of these chambers. Additionally, Selamet et al. [52] explored the effect of perforated ducts on sound attenuation in dissipative silencers, further advancing our understanding of these systems. Nawaz and Lawrie, [39] as well as Nawaz et al. [37], examined the scattering of sound waves at a finite junction with structural discontinuity and obstacles. Their approach employed continuity conditions for pressure and normal velocities at the aperture to match the scattering modes. In a related study, Afzal et al. [5] investigated a two-dimensional reactive silencer design, featuring a membrane attached to the internal walls of the expansion chamber and an elastic plate parallel to the inlet/outlet axis, attached to the outlet duct. This design aims to enhance sound attenuation and acoustic performance.

Accordingly, the mode-matching method has been applied to scattering problems in [2, 3, 6–8, 29, 38, 40, 41, 53]. Lawrie [27] established a class of orthogonality relations crucial for understanding fluid-structure interaction. Haung [20] investigated the acoustic behavior of drum-like silencers and sound wave reflection within chambers enclosed by vertical plates. Additionally, Satti et al. [50] examined the performance of expansion chamber silencers featuring membrane-bound cavities and horizontal partitions. The study considered various surface conditions for the splitting walls, including rigid, soft, impedance, and sound-absorbing materials, to understand their impact on silencer performance. Rienstra [49] conducted a thorough analysis of the acoustic modes in a lined channel, both with and without uniform mean flow. His work revealed the existence of three distinct types of modes: genuine acoustic modes, acoustic surface waves, and hydrodynamic surface waves.

Brambley and Peake [13] further investigated the behavior of these surface modes. It is important to note that, in the presence of flow, viscosity effects become significant near the walls, necessitating the consideration of boundary layers. Hassan and Rawlins [48] explored sound radiation in a trifurcated waveguide, solving a mathematical problem with Robin-type boundary conditions on some surfaces and rigid conditions on others. Ayub et al. [9] provided a solution to the diffraction problem in an acoustical trifurcated waveguide with mean flow, featuring hard and soft parallel planes and half-planes. Meanwhile, Wang and Mak [60] explored

sound wave propagation in a lined duct with periodic resonators array. In a related study, Afzal et al. [4] examined wave dissipation in a discontinuous flexible waveguide. Additionally, Lawrie and Abrahams discussed generalized orthogonal properties of boundary value problems, encompassing higher-order boundary conditions, further advancing our understanding of these complex acoustic systems. This research has significant implications for noise reduction and has been extensively investigated by various authors. Miles [34] early study on acoustic scattering in a rigid, cylindrical duct laid the groundwork for future research. Chenxi Li [31] discuss the Acoustic impedance of micro perforated membranes: Velocity continuity condition at the perforation boundary .Building on this foundation, Levine and Schwinger [30] derived a closed-form solution for the reflection coefficient in a semi-infinite, rigid, cylindrical duct, providing an exact solution to the problem. Ingard [22] further expanded our understanding by examining the sound radiation characteristics of a plane piston at the end of a finite, rigid, open cylindrical duct. This work involved analyzing the acoustic pressure field at the duct's open end, which is typically governed by Helmholtz or Laplace-type differential equations, subject to various boundary conditions (Dirichlet, Neumann, or Robin types). These contributions have collectively advanced our knowledge of acoustic behavior in ducts, informing strategies for effective noise reduction. A range of analytical and numerical methods have been developed to tackle various problems for instance [10, 12, 17, 26, 28, 51, 58].

1.2 Thesis Structure

The present thesis include five chapters.

- **Chapter 1** provides an introduction to the research presented in this thesis, accompanied by a comprehensive literature review that investigate and informs the work undertaken. This chapter sets the stage for the investigation that follows, providing a foundation in the relevant theoretical and empirical knowledge that has shaped the research questions and objectives.

- **Chapter 2** comprises some basic definitions, physical laws and formulation of wave equation.

- **Chapter 3** contains the propagation of acoustic waves from a membrane panel in a waveguide radiated by a planar wave.

- **Chapter 4** contains the propagation of acoustic waves from a membrane panel in a waveguide emitted by a planar piston.

- **Chapter 5** provides the concluding remarks of the present study.

The references used in the thesis are mentioned in **Bibliography**.

Chapter 2

Preliminaries

This chapter contains some basic definitions and governing laws, which will be helpful in the subsequent chapters.

2.1 Acoustic [57]

The field of acoustics has undergone a remarkable evolution since its inception, starting with the study of audible sound waves and expanding to include a broad spectrum of frequencies and applications. From structural and environmental acoustics to bioacoustics and beyond, it encompasses a wide array of disciplines such as physics, engineering, and music.

2.2 Acoustic Wave Equation [32]

The behavior of acoustic waves in a medium, such as air, can be described using mathematical equations that are derived from fundamental physical principles, including conservation of mass, momentum, and energy. However, these equations are often nonlinear and complex, making them difficult to analyze. To overcome this challenge, a linear approximation is commonly used, which simplifies the

equations and allows for a more straightforward analysis of the wave propagation, providing valuable insights into the behavior of acoustic waves in the medium.

2.2.1 Conservation of Mass [14]

The conservation of mass equation represents the relationship between the rate of change of mass density and the net flow of mass into or out of a given volume, per unit time that is

$$\frac{\partial \rho}{\partial t} + \bigtriangledown.(\rho u) = 0, \tag{2.1}$$

where u shows flow velocity and ρ represents instantaneous of mass density.

2.2.2 Conservation of Momentum [56]

The conservation of momentum equation associate the net momentum flowing per unit time to the forces acting on it.

$$\frac{\partial \rho u}{\partial t} = - \bigtriangledown .(\rho u)u - \bigtriangledown p + \rho g, \tag{2.2}$$

where, p is the pressure, g is gravitational acceleration, $\bigtriangledown p$ denotes the exerting force and ρg shows the body force. From the above equation (2.1),

$$\frac{\partial \rho u}{\partial t} + \bigtriangledown.(\rho u)u = - \bigtriangledown p + \rho g, \tag{2.3}$$

which implies that

$$\left(\frac{\partial \rho}{\partial t} + \bigtriangledown.(\rho u)\right) u = \rho \left(\frac{\partial}{\partial t} + u.\bigtriangledown\right) u = - \bigtriangledown p + \rho g. \tag{2.4}$$

By using the continuity condition, we can write

$$\rho \frac{Du}{Dt} = - \bigtriangledown p + \rho g, \tag{2.5}$$

where $\frac{D}{Dt} = \frac{\partial}{\partial t} + u.\bigtriangledown$ is the total time derivative known as Stokes total time derivative contain first term to be time derivative and second term the convective term.

2.2.3 Equation of State [55]

The thermodynamic behaviour of compressible fluid can be defined by the equation of state. For the perfect gas, the equation of state is

$$p = \rho r T, \tag{2.6}$$

where T used for temperature, and r gives specific gas constant. For a gas enclosed in a vessel of highly thermally conductive walls, the perfect gas isotherm can be given by

$$\frac{p}{p_0} = \frac{\rho}{\rho_0}, \tag{2.7}$$

where ρ_0 and p_0 are the static density and pressure respectively. When no heat loss or gained by the system then perfect adiabatic is

$$\frac{p}{p_0} = \left(\frac{\rho}{\rho_0}\right)^{\gamma}, \tag{2.8}$$

where, γ is the ratio of specific heat at constant pressure C_p to the specific heat at constant volume C_v i.e, $\gamma = \frac{C_p}{C_v}$ =Ratio of heat capacities. The compression and rarefaction in a gas can be defined as condensation i.e

$$s = \frac{\rho - \rho_0}{\rho_0}, \tag{2.9}$$

which yields

$$\rho = \rho_0(1 + s). \tag{2.10}$$

By using (2.10) into (2.8) we found

$$\frac{p}{p_0} = (1 + s)^{\gamma}. \tag{2.11}$$

Expanding the right hand side of above equation by using Taylor's series

$$\frac{p}{p_0} = 1 + \gamma s + \frac{\gamma(\gamma-1)}{2fic}s^2 + ... \tag{2.12}$$

For linear relationship

$$\frac{p}{p_0} \approx 1 + \gamma s + O(s^2), \tag{2.13}$$

or

$$\frac{p}{p_0} \approx 1 + \gamma s, \tag{2.14}$$

or

$$p - p_0 = \gamma p_0 s. \tag{2.15}$$

Another way to determine the adiabatic relationship between pressure and density fluctuations is by using a Taylor series expansion of the pressure around the equilibrium density can also be written as

$$p = p(\rho_0) + \left(\frac{\partial p}{\partial \rho}\right)_{\rho=\rho_0}(\rho - \rho_0) + \left(\frac{\partial^2 p}{\partial \rho^2}\right)_{\rho=\rho_0}(\rho - \rho_0).... \tag{2.16}$$

or

$$p \approx p(\rho_0) + \left(\frac{\partial p}{\partial \rho}\right)_{\rho=\rho_0}(\rho - \rho_0), \tag{2.17}$$

or

$$p - p_0 = \left(\frac{\partial p}{\partial \rho}\right)_{\rho=\rho_0}(\rho - \rho_0). \tag{2.18}$$

Now comparing equation (2.15) and (2.18) we found

$$\gamma = \frac{\beta}{\rho}. \tag{2.19}$$

where, $\beta = \rho_0(\frac{\partial p}{\partial \rho})_{\rho=\rho_0}$, the acoustic pressure at any point can be defined as,

$$P = p - p_0. \tag{2.20}$$

Additionally, Equation (2.18) allows us to define the acoustic pressure as:

$$P = \beta s. \tag{2.21}$$

2.2.4 Acoustic Membrane[19]

In acoustic waveguides, a membrane can be a thin plate or a diaphragm that vibrates in response to sound waves, affecting the wave propagation. Membranes can be used to:

- Separate different sections of the waveguide
- Introduce discontinuities or obstacles
- Enhance or suppress specific frequency ranges
- Create filters or resonators

Membranes play a crucial role in shaping the wave behavior, scattering, and transmission within the waveguide.

2.2.5 Micro-Perforated Acoustic Membrane [47]

A micro perforated elastic membrane is a thin, flexible sheet with tiny holes (micro perforations) that allow for acoustic energy to pass through while maintaining its structural integrity. This design enables the membrane to absorb sound energy effectively, making it a popular choice for various acoustic applications, such as:

- Sound Absorption Panels
- Acoustic Filters
- Silencers
- Soundproofing Materials

The micro perforations create a large surface area, allowing for enhanced sound energy dissipation, while the elastic properties of the membrane enable it to withstand mechanical stress and maintain its shape.

2.3 Impedance Conditions

2.3.1 Soft Conditions [33]

The soft boundary conditions are Drichlet's type boundary conditions. In these type of conditions, the pressure or displacement is consider as zero, i.e.

$$\psi(x, y) = 0$$

.

2.3.2 Rigid Conditions [24]

Neumann's type boundary conditions are actually rigid boundary conditions. In rigid conditions, normal velocity is consider as zero, i.e.

$$\frac{\partial \psi}{\partial x} = 0$$

2.3.3 Edge Conditions [59]

Edge conditions in a waveguide are the boundaries or constraints imposed on the wavefield at the edges, determining how the wave behaves, such as reflection, absorption, or transmission. Common edge conditions include hard wall, soft wall, periodic, absorbing, and impedance boundaries.

2.3.4 Spring-Like Conditions [61]

Spring-like conditions in a waveguide or acoustic system are boundaries that:

- Allow displacement in response to force (pressure)

- Return to their original position when the force is removed
- Do not dissipate energy (no damping)

2.3.5 Fixed Conditions [11]

In a waveguide, a fixed condition, also known as a "fixed boundary" or "clamped boundary", is a boundary where:

- The displacement (movement) is zero
- The wavefield is not allowed to move or vibrate
- The boundary is rigid and immovable

2.3.6 Free Conditions [18]

In a waveguide, a free condition, also known as a "free boundary" or "unbounded boundary", is a boundary where:

- The wavefield is allowed to move or vibrate freely
- There are no constraints on the displacement (movement)
- The boundary is not rigid or fixed

2.4 Basic Definitions [32]

2.4.1 Waveguides

Waveguides are structures designed to guide waves, such as electromagnetic waves or sound, while minimizing energy loss by constraining their expansion to one or

two dimensions. The shape and design of a waveguide determine its function, with acoustics waveguides behaving similarly to transmission lines, facilitating the propagation of sound waves within them.

2.4.2 Amplitude

Amplitude refers to the maximum magnitude or intensity of a wave, oscillation, or signal. In various contexts, amplitude can describe:

- Sound waves: The loudness or intensity of a sound.
- Light waves: The brightness or intensity of light.
- Electrical signals: The voltage or current level of an electrical signal.
- Vibrations: The magnitude of oscillations or vibrations.
- Mathematical functions: The maximum value of a function.

In general, amplitude represents the "size" or "strength" of a wave or signal, often measured from its equilibrium or zero point to its peak value.

2.4.3 Time Period

The time taken by the vibrating object to complete one cycle of motion is called time period. The period of oscillation is also known as the time period and is denoted by T

$$T = \frac{2\pi}{\omega}. \tag{2.22}$$

2.4.4 Frequency

Frequency refers to the number of oscillations or cycles of a wave, signal, or vibration per unit time. It is typically measured in units of hertz (Hz), where 1 Hz equals one cycle per second. Frequency is a fundamental property of waves and signals, and it plays a crucial role in various fields, including:

- Sound: Pitch and tone
- Light: Color and spectrum
- Electrical engineering: AC circuits and signal processing
- Vibrations: Mechanical resonance and structural analysis
- Physics: Wave behavior and quantum mechanics

Frequency is often represented by the symbol "f" and is related to other wave properties, such as wavelength and amplitude, through the speed of the wave.

2.5 Mode-Matching Scheme [35]

Various analytical approaches have been devised to study the reflection, transmission, and absorption of waves in waveguides. The selection of these strategies depends on the material and geometrical properties of the guiding structures, as well as the underlying physical principles governing the system. Among these methods, the Mode-Matching (MM) technique is particularly widely used for problems involving structural discontinuities and non-uniform impedance distributions along the surfaces. The MM technique has proven effective in handling such complexities, making it a popular choice in the field.

The Mode-Matching (MM) technique is a numerical method that solves acoustic problems by dividing the guiding structure into segments and determining the field

potentials within each segment. The potentials are expanded in terms of unknown amplitudes, which are then determined by matching pressures and velocities at the interfaces between segments. The differential system is converted into a linear algebraic framework, enabling the truncation and solution of the resulting equations to obtain the unknown amplitude coefficients. The MM technique has a wide range of applications in solving physical problems, including those in the automobile industry, heating, ventilation, and air conditioning (HVAC) systems in buildings, and various engineering structures. Its versatility and accuracy make it a valuable tool in these fields.

In the HVAC and automobile industries, duct-like structures play a crucial role in transferring vibrational energy, which can sometimes manifest as noise. Therefore, designing these elements to minimize noise is essential. Such designs often involve various geometric modifications and material properties within the structures. However, solving the governing boundary value problems associated with these physical systems can be challenging. Fortunately, the Mode-Matching (MM) technique offers a relatively straightforward approach to finding solutions to these problems. This technique provides an attractive method for tackling these challenges, and some examples of its applications are discussed in Chapters 3 and 4.

Chapter 3

The Propagation of Acoustic Waves from a Membrane Panel in a Waveguide Radiated by a Planar Wave

In this chapter, we study acoustic propagation and scattering along membrane interface and a plane wave is incident on a membrane positioned at the center of an infinite waveguide. The governing boundary value problems (BVPs) contain Helmholtz equation, rigid conditions, membrane condition and edge conditions. The eigenfunctions in given duct regions are orthogonal in nature.

Eigenfunction expansions are derived, and matching conditions are applied to obtain linear algebraic systems. The matching conditions as well as with well defined orthogonal characteristics lead to the solution of the problem. The process is discussed comprehensively in following sections. In section 3.1, the scattering through the membrane interface in a continuous duct is given.

3.1 Scattering Through Membrane Interface in Continuous Duct

Consider an infinite cylindrical waveguide with radius $\bar{r} = \bar{a}$, having membrane at $\bar{z} = 0$, as shown in Fig. 3.1. An overbar with a variable expresses the dimensional setting. The inner side of waveguide is filled with compressible

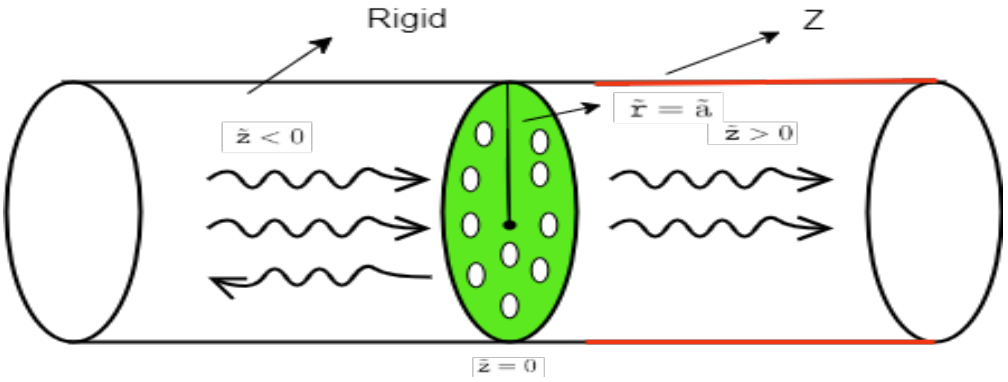

FIGURE 3.1: The physical configuration of waveguide.

fluid of density ρ and sound speed c. The region at $\bar{z} \leq 0$ is bounded by rigid surface while the semi-infinite region at $\bar{z} \geq 0$ contains impedance type condition on $\bar{r} = \bar{a}$. The fluid potential in waveguide satisfies the dimensional wave equation

$$\bar{\nabla}^2 \Phi(\bar{r}, \bar{z}, \bar{t}) - \frac{1}{c^2} \frac{\partial \bar{\Phi}^2}{\partial \bar{t}^2} = 0. \tag{3.1}$$

The fluid potential $\bar{\Phi}$ is related to acoustic pressure $\bar{P}$ and velocity vector $\bar{\mathbf{V}}$ through the relations:

$$\bar{P} = \rho \frac{\partial \bar{\Phi}}{\partial \bar{t}}, \tag{3.2}$$

and

$$\bar{\mathbf{V}} = \bar{\nabla} \bar{\Phi}, \tag{3.3}$$

respectively. At $\bar{z} \leq 0$ bounding wall of waveguide is consider acoustically rigid. The boundary conditions for acoustically rigid surface is

$$\frac{\partial \bar{\Phi}}{\partial \bar{r}} = 0, \quad \bar{r} = \bar{a}. \tag{3.4}$$

Whereas, at $\bar{z} \geq 0$, the impedance condition is

$$-\rho\frac{\partial\bar{\Phi}}{\partial\bar{t}} - \bar{z}\frac{\partial\bar{\Phi}}{\partial\bar{z}} = 0, \tag{3.5}$$

where $\bar{z}$ express the dimensional surface impedance. At $\bar{z} = 0$, there is located a circular membrane disc. The equation of motion the membrane disc as given is [31]

$$T\bar{\nabla}^2\bar{W}(\bar{r}) - \rho_m\frac{\partial^2\bar{W}(\bar{r})}{\partial\bar{t}^2} = (\bar{P}^+ - \bar{P}^-), \tag{3.6}$$

where T denotes the tension in membrane having density ρ_m. Here $\bar{P}^+$ denotes the dimensional pressure for the region $\bar{z} \geq 0$. while $\bar{P}^-$ represents the pressure in the region where $\bar{z} \leq 0$. Here $\bar{W}(\bar{r})$ denotes the displacement in circular membrane. However, if the membrane is perforated that contain tiny circular holes, then the equation of motion as given in [23] is

$$T\bar{\nabla}^2\bar{W}(\bar{r}) - 2\tilde{\eta}\frac{\partial(\bar{\nabla}^2\bar{W})}{\partial\ \bar{t}} - \rho_m\frac{\partial^2\bar{W}(\bar{r})}{\partial\bar{t}^2} = (\bar{P}^+ - \bar{P}^-), \tag{3.7}$$

where $\tilde{\eta}$ denotes the damping of the membrane. Note that for circular disc we consider

$$\bar{\nabla}^2 = \frac{\partial^2}{\partial r^2} + \frac{1}{r}\frac{\partial}{\partial r}, \tag{3.8}$$

and

$$\frac{\partial\bar{\Phi}}{\partial\bar{z}} = \frac{\partial\bar{W}}{\partial\bar{t}}. \tag{3.9}$$

On considering the harmonic time dependence $e^{-i\omega\bar{t}}$, we write

$$\left.\begin{aligned}\bar{\Phi}(\bar{r},\bar{z},\bar{t}) &= \bar{\phi}(\bar{r},\bar{z})e^{-i\omega\bar{t}},\\ \bar{W}(\bar{r},\bar{t}) &= \bar{w}(\bar{r})e^{-i\omega\bar{t}},\\ \bar{P}(\bar{r},\bar{z},\bar{t}) &= \bar{p}(\bar{r},\bar{z})e^{-i\omega\bar{t}},\\ \bar{V}(\bar{r},\bar{z},\bar{t}) &= \bar{v}(\bar{r},\bar{z})e^{-i\omega\bar{t}}.\end{aligned}\right\} \tag{3.10}$$

Further, we transform the problem into dimensionless form using transformation

$$\left.\begin{aligned} k\bar{r} &= r, \\ k\bar{z} &= z, \\ t &= \omega\bar{t}, \\ k^2\bar{\Phi} &= \omega\phi, \\ k\bar{W} &= w. \end{aligned}\right\} \tag{3.11}$$

Here k assumes the dimension of length inverse $[L]^{-1}$ and w of time inverse $[T]^{-1}$. Here r, z, w and ϕ are dimensionless quantities. By using (3.11), (3.1) gives the Helmholtz's equation of non-dimensional form as:

$$\left(\frac{\partial^2}{\partial r^2} + \frac{1}{r}\frac{\partial}{\partial r} + \frac{\partial^2}{\partial z^2} + 1\right)\phi(r, z) = 0, \tag{3.12}$$

where ϕ is the dimensionless potential that with reference to duct region I and II can be written as:

$$\phi = \begin{cases} \phi_1(r, z), & z < 0, \quad 0 \leq r \leq a, \\ \phi_2(r, z), & z > 0, \quad 0 \geq r \geq a. \end{cases} \tag{3.13}$$

The membrane equations at $z = 0$, in dimensionless form with and without perforation can be given as follow:

- For the membrane without micro-perforated holes

$$\left(\frac{\partial^2}{\partial r^2} + \frac{1}{r}\frac{\partial}{\partial r} + \mu^2\right) w = \alpha(\phi_2 - \phi_1), \tag{3.14}$$

where

$$\alpha = \frac{c_m^2\rho}{KT}, \quad \text{and} \quad \mu = \frac{c_m\sqrt{\rho_m}}{\sqrt{T}}, \tag{3.15}$$

are fluid loading parameter and membrane wave number respectively, where c_m is the sound's speed on membrane.

- For the membrane with micro-perforated holes

$$\left(\frac{\partial^2}{\partial r^2}+\frac{1}{r}\frac{\partial}{\partial r}+\tilde{\mu}^2\right)\tilde{w}=\tilde{\alpha}(\phi_2-\phi_1), \tag{3.16}$$

where

$$\tilde{\alpha}=\frac{c_m^2\rho_0}{KT+i\eta k^2 c_m}, \quad \text{and} \quad \tilde{\mu}=\frac{c_m\sqrt{\rho_m}}{\sqrt{T+i\eta c_m k}} \tag{3.17}$$

are dimensionless parameters. At the rim where membrane is attached to the cylinder the spring-like condition is

$$w^{'}(a)+\xi w(a)=0. \tag{3.18}$$

where $\xi=k\bar{\xi}$ is coupling parameter. The rigid and impedance boundary condition in dimensionless form are

$$\frac{\partial\phi_1}{\partial r}=0, \quad r=a, \quad z<0, \tag{3.19}$$

and

$$\phi_2-i\mathcal{Z}\frac{\partial\phi_2}{\partial r}=0, \quad r=a, z>0, \tag{3.20}$$

where $\mathcal{Z}$ is the dimensionless surface impedance. Further, the normal velocities $z=0$ are continuous, that gives

$$\frac{\partial\phi_1}{\partial z}=\frac{\partial\phi_2}{\partial z}, \qquad \text{at} \quad z=0, \quad 0<r<a. \tag{3.21}$$

Suppose an incident wave strikes at membrane, a part is reflected in region I while rest is transmitted into the region II. We solve the governing boundary value problem by using mode-matching technique to analyze the reflection and transmission. The solution is explained in next section.

3.2 Mode-Matching Solution

In this method, to determine the eigenfunctions expansion of fluid potential in duct regions I and II, first we apply the separation of variable method. For region I, we consider

$$\phi_1(r,z)=R_1(r)Z_1(z). \tag{3.22}$$

By using (3.22) into (3.12), we get

$$\frac{R_1''}{R_1} + \frac{1}{r}\frac{R_1'}{R_1} + 1 = -\frac{Z_1''}{Z_1} = \nu^2(\text{say}). \tag{3.23}$$

From (3.23), the solution of ordinary differential equation for $Z_1(z)$ is

$$Z_1(z) = c_1 e^{i\eta z} + c_2 e^{-i\eta z}, \tag{3.24}$$

whereas, the ordinary differential equation for $R_1(r)$ is

$$r^2 R_1'' + r R_1' + r^2\tau^2 R_1 = 0 \quad \text{with} \quad r = \sqrt{1-\nu^2}, \tag{3.25}$$

which is a Bessel differential equation. The solution of equation (3.25) is

$$R_1 = c_3 J_0(\tau r) + c_4 N_0(\tau r), \tag{3.26}$$

where $J_0(\tau r)$ and $N_0(\tau r)$ are Bessel functions of first and second kinds respectively, and c_1 and c_2 are arbitrary constants. It is compulsory to note that when $r \to 0$ the Bessel functions of second kind becomes undefined so, we choose $c_4 = 0$ for bounded solution, and (3.26) becomes

$$R_1(r) = c_3 J_0(\tau r). \tag{3.27}$$

Now we have to find c_3 so, we put (3.25) into boundary condition (3.19). As the bounding surface is acoustically rigid, therefore from (3.19) and (3.26), we get

$$R_1'(a) = 0, \tag{3.28}$$

or

$$J_0'(\tau a) = 0, \tag{3.29}$$

which is dispersion relation for τ. From (3.29) we get infinitely many values for $\tau = 0$ such that $\tau \equiv \tau_n$, $n = 0, 1, 2, \cdots$ and eigenfunctions

$$R_1 \equiv R_{1n}(r) = J_0(\tau_n r), \quad \text{for} \quad n = 0, 1, 2, \cdots \tag{3.30}$$

where, for $\tau = \tau_n$, the mode wavenumber $\eta \equiv \eta_n = \sqrt{1-\tau_n^2}$, and (3.22) gives

$$\phi_{1n} = A_n R_{1n}(r) e^{i\eta_n z} + B_n R_{1n}(r) e^{-i\eta_n z}. \tag{3.31}$$

Note that first term of right hand side of (3.31) gives the expression for n^{th} propagating mode towards positive direction and second term on right hand sides stands for the n^{th} mode propagation in negative z-direction. The coefficients A_n and B_n are amplitudes of n^{th} propagating modes. From superposition principle, the total field potential in region I can be given as:

$$\phi_1(r,z) = \sum_{n=0}^{\infty} \phi_{1n}(r,z), \tag{3.32}$$

or

$$\phi_1(r,z) = \sum_{n=0}^{\infty} (A_n e^{i\eta_n z} + B_n e^{-i\eta_n z}) R_{1n}(r). \tag{3.33}$$

Same as for region II, we solve the following equation

$$\left(\frac{\partial^2}{\partial r^2} + \frac{1}{r}\frac{\partial}{\partial r} + \frac{\partial^2}{\partial z^2} + 1 \right) \phi_2(r,z) = 0, \tag{3.34}$$

subject to boundary condition

$$\phi_2 - i\mathcal{Z}\frac{\partial \phi_2}{\partial r}(a,z) = 0, \tag{3.35}$$

and get

$$\phi_2(r,z) = \sum_{n=0}^{\infty} (C_n e^{i\nu_n z} + D_n e^{-i\nu_n z}) R_{2n}(r), \tag{3.36}$$

where

$$R_{2n}(r) = J_0(\gamma_n r); \quad \nu_n = \sqrt{1-\gamma_n^2}, \tag{3.37}$$

and γ_n are the roots of dispersion relation

$$J_0(\gamma_n a) - i\mathcal{Z} J_0'(\gamma_n a) = 0. \tag{3.38}$$

Here $\{A_n, B_n, C_n, D_n\}$ are unknowns in (3.33) and (3.36). From region I, we take the fundamental duct mode with unit amplitude to positive z-direction, by setting

$A_n = \delta_{n0}$ in (3.33). Moreover we consider only transmission in region II by setting $D_n = 0$ in (3.36). So, from (3.33) and (3.36) we get

$$\phi_1(r,z) = e^{iz} + \sum_{n=0}^{\infty} B_n R_{1n}(r) e^{-i\eta_n z}, \tag{3.39}$$

$$\phi_2(r,z) = \sum_{n=0}^{\infty} C_n R_{2n}(r) e^{i\nu_n z}. \tag{3.40}$$

Here B_n representing the reflected mode amplitudes and C_n representing the transmitted mode amplitudes are still unknown for $n = 0, 1, 2, \cdots$. These are found by using mode-matching procedure. This method requires orthogonality and matching conditions. First, we explain the orthogonality condition for eigenfunctions R_{2n} where $n = 0, 1, 2, \cdots$.

3.2.1 Orthogonality Relation with Impedance Condition for Region-II

Here we derive orthogonality relation for impedance involving condition. The orthogonality relation for rigid problem can be treated as a subcase of the impedance setting. From (3.34) and (3.35), the eigen value problem for the region at $z > 0$ can given as:

$$R''_{2n}(r) + \frac{1}{r} R'_{2n}(r) = -{\tau_n}^2 R_{2n}(r), \tag{3.41}$$

$$R_{2n}(a) - i\mathcal{Z} R'_{2n}(a) = 0. \tag{3.42}$$

Multiplying (3.42) with $aR_{2m}(a)$ to find orthogonality relation, we get

$$a[R_{2m}(a)R_{2n}(a) - i\mathcal{Z} R'_{2n}(a)R_{2m}(a)] = 0. \tag{3.43}$$

By swapping n by m we find

$$a[R_{2n}(a)R_{2m}(a) - i\mathcal{Z} R'_{2m}(a)R_{2n}(a)] = 0. \tag{3.44}$$

On subtracting (3.43) from (3.44), it is clearly derive that

$$a[R_{2n}(a)R_{2m}(a) - i\mathcal{Z}R'_{2m}(a)R_{2n}(a)] - a[R_{2m}(a)R_{2n}(a) - i\mathcal{Z}R'_{2n}(a)R_{2m}(a)] = 0, \tag{3.45}$$

or

$$r[(R_{2n}(r)R_{2m}(r) - i\mathcal{Z}R'_{2m}(r)R_{2n}(r)) - r(R_{2m}(r)R_{2n}(r) - i\mathcal{Z}R'_{2n}(r)R_{2m}(r))]_{r=0}^{r=a} = 0. \tag{3.46}$$

By differentiating with respect to r, taking the integral, as well, the (3.46) can be written as

$$\begin{aligned} &\int_0^a \frac{d}{dr} r[(R_{2n}(r)R_{2m}(r) - i\mathcal{Z}R'_{2m}(r)R_{2n}(r)) - r(R_{2m}(r)R_{2n}(r) \\ &- i\mathcal{Z}R'_{2n}(r)R_{2m}(r))]dr = 0, \end{aligned} \tag{3.47}$$

which on simplification leads to

$$\int_0^a [r(R_{2n}(r)(R''_{2m}(r) + \frac{1}{r}R'_{2m}(r)) - rR_{2m}(r)(R''_{2n}(r) + \frac{1}{r}R'_{2n}(r))]dr = 0. \tag{3.48}$$

By using (3.41) and (3.48), leads to

$$(\tau_n^2 - \tau_m^2)\int_0^a R_{2m}(r)R_{2n}(r)rdr = 0. \tag{3.49}$$

If $(\tau_n^2 - \tau_m^2) \neq 0$, then (3.49) leads to

$$\int_0^a R_{2m}(r)R_{2n}(r)rdr = 0. \tag{3.50}$$

If $(\tau_n^2 - \tau_m^2)$=0, then integral takes the form

$$\int_0^a R_{2m}(r)R_{2n}(r)rdr = \int_0^a R_{2n}^2(r) = F_{2n}, \tag{3.51}$$

where

$$F_n = \frac{a^2}{2}J_0^2(\tau_n a). \tag{3.52}$$

On combining (3.50) and (3.51), we get

$$\int_0^a R_{2m}(r)R_{2n}(r)rdr = \delta_{mn}F_{2n}, \tag{3.53}$$

where δ_{mn} is Kronecker delta, that is

$$\delta_{mn} = \begin{cases} 0 & m \neq n, \\ 1 & m = n. \end{cases} \tag{3.54}$$

3.2.2 Orthogonality Relation with Impedance Condition for Region-I

For eigenvalues ν_n and eigenfunction $R_{1n} = J_0(\nu_n r)$, the related eigenvalue problem is

$$R''_{1n}(r) + \frac{1}{r}R'_{1n}(r) = -{\nu_n}^2 R_{1n}(r), \tag{3.55}$$

$$R'_{1n}(a) = 0, \tag{3.56}$$

On adopting the same procedure as explained to get the orthogonality relation for region-II, we can find the following form of orthogonality relation for region-I

$$\int_0^a R_{1m}(r)R_{1n}(r)rdr = \delta_{mn}F_n, \tag{3.57}$$

where

$$\int_0^a R_{1n}^2(r) = F_{1n}. \tag{3.58}$$

Once the orthogonality relation is proved, we can apply the interface conditions to find B_n and C_n. Now we use the membrane condition at $z = 0$, to determine unknowns B_n and C_n, we rewrite (3.14) as follows

$$\left(\frac{\partial^2}{\partial r^2} + \frac{1}{r}\frac{\partial}{\partial r} + \mu_m^2\right)\frac{\partial \phi_1}{\partial z} + \alpha_m \phi_1 = \alpha_m \phi_2 + \frac{\delta(r-a)}{r}E_1. \tag{3.59}$$

On using (3.39) and (3.40) into (3.59), we get

$$\sum_{n=0}^{\infty} B_n \Delta_n R_{1n} + (i\mu_m^2 + \alpha_m) = \alpha_m \sum_{n=0}^{\infty} C_n R_{2n}(r) + \frac{\delta(r-a)}{r} E_1, \tag{3.60}$$

$$\Delta_n = -i\eta_n(-{\tau_n}^2 + {\mu_m}^2) + \alpha_m. \tag{3.61}$$

Multiplying (3.61) with $rR_{1m}(r)$ and integrating $0 \leq r \leq a$, we get

$$\begin{aligned} &\sum_{n=0}^{\infty} B_n \Delta_n \int_0^a R_{1n} R_{1m} r dr + (i\mu_m^2 + \alpha_m) \int_0^a R_{1m} r dr \\ &= \alpha_m \sum_{n=0}^{\infty} C_n \int_0^a R_{1m} R_{2n} r dr + E_1 \int_0^a \frac{\delta(r-a)}{r} R_{1m}(r) r dr, \end{aligned} \tag{3.62}$$

which on using orthogonality relation (3.53), we get

$$\sum_{n=0}^{\infty} B_n \Delta_n \delta_{mn} F_n = -(i\mu_m^2 + \alpha_m)\delta_{m0} F_m + \alpha_m \sum_{n=0}^{\infty} C_n P_{nm} + E_1 R_{1m}(a). \tag{3.63}$$

On making some mathematical rearrangements which leads to

$$B_m = \frac{-(i\mu_m^2 + \alpha_m)\delta_{m0}}{\Delta_m} + \frac{\alpha_m}{\Delta_m F_m} \sum_{n=0}^{\infty} C_n P_{nm} + \frac{E_1 R_{1m}(a)}{F_m \Delta_m}. \tag{3.64}$$

Here, constant E_1 is unknown and it will be found through some condition on rim at $r = a$. For sake of generality, we consider spring like condition (3.18), which on using $w = \frac{\partial \phi_1}{\partial z}$ becomes

$$\frac{\partial^2 \phi_1}{\partial r \partial z} + \xi \frac{\partial \phi_1}{\partial z} = 0. \tag{3.65}$$

On using (3.39) into (3.65), we get

$$\xi - \sum_{n=0}^{\infty} B_n \eta_n \left(R'_{1n}(a) + \xi R_{1n}(a) \right) = 0. \tag{3.66}$$

From (3.64), we have

$$B_n = \frac{-(i\mu_n^2 + \alpha_n)\delta_{n0}}{\Delta_n} + \frac{\alpha}{\Delta_n F_n}\sum_{p=1}^{\infty} C_p P_{np} + \frac{E_1 R_{1n}(a)}{F_n \Delta_n}. \tag{3.67}$$

Using (3.67) into (3.66), we find values of constant E_1 as:

$$\begin{aligned} \xi - \sum_{n=0}^{\infty}\left(\frac{-(i\mu_n^2 + \alpha_n)\delta_{n0}}{\Delta_n} + \frac{\alpha}{\Delta_n F_n}\sum_{p=1}^{\infty} C_p P_{np} + \frac{E_1 R_{1n}(a)}{F_n \Delta_n}\right) \\ \eta_n \left(R'_{1n}(a) + \xi R_{1n}(a)\right) = 0, \end{aligned} \tag{3.68}$$

simplification leads to

$$\begin{aligned} E_1 = \frac{\xi}{S} + \frac{1}{S}\left(\frac{(i\mu_0^2 + \alpha_0)\eta_0(R'_{10}(a) + \xi R_{10}(a))}{\Delta_0}\right) \\ - \frac{\alpha}{S}\sum_{n=0}^{\infty}\sum_{p=0}^{\infty}\frac{C_p P_{np}\eta_n(R'_{1n}(a) + \xi R_{1n}(a))}{F_n \Delta_n}, \end{aligned} \tag{3.69}$$

where

$$S = \sum_{n=0}^{\infty}\frac{\eta_n R_{1n}(R'_{1n}(a) + \xi R_{1n}(a))}{F_n \Delta_{1n}}, \tag{3.70}$$

Now on using (3.39) and (3.40) into (3.21), we found

$$\sum_{n=0}^{\infty} C_n \nu_n R_{2n}(r) = 1 - \sum_{n=1}^{\infty} B_n \eta_n R_{1n}(r). \tag{3.71}$$

Multiplying by rR_{2m} and integrating from 0 to a with (3.71), we get

$$\sum_{n=0}^{\infty} C_n \nu_n \int_0^a R_{2m}R_{2n}rdr = \int_0^a R_{2m}R_{2n}rdr - \sum_{n=1}^{\infty} B_n \eta_n \int_0^a R_{2m}R_{2n}rdr, \tag{3.72}$$

on using orthogonality relation (3.53), we get

$$C_m = \frac{1}{\nu_n F_{2m}}\left(P_{0m} - \sum_{n=1}^{\infty} B_n \eta_n P_{nm}\right). \tag{3.73}$$

3.3 Energy Expression

To analyze problem physically, the dimensional energy flux can be defined as

$$\mathcal{E} = 2\pi\omega\rho Re\Big[\int_{\Omega} i\bar{\phi}\left(\frac{\partial\bar{\phi}}{\partial\bar{z}}\right)^{*}\bar{r}d\bar{r}\Big], \tag{3.74}$$

where Ω is the region. By non-dimensionalizing under the transformation given in (3.1), we get

$$\mathcal{E} = \frac{2\pi\omega^3\rho}{k^5}Re\Big[\int_{\Omega} i\phi(\frac{\partial\phi}{\partial z})^{*}rdr\Big], \tag{3.75}$$

By using $\omega = ck$ in equation (3.75), we find

$$\mathcal{E} = \frac{2\pi c^3\rho}{k^2}Re\Big[\int_{\Omega} i\phi\left(\frac{\partial\phi}{\partial z}\right)^{*}rdr\Big]. \tag{3.76}$$

That gives non-dimensional energy flux

$$\mathcal{E} = Re\Big[\int_{\Omega} i\phi\left(\frac{\partial\phi}{\partial z}\right)^{*}rdr\Big], \tag{3.77}$$

where $\mathcal{E} = \frac{k^2\bar{\mathcal{E}}}{2\pi c^3\rho}$. Now by using incident field as $\phi_{inc} = e^{iz}$, (3.77) leads to incident power

$$\mathcal{E}_{inc} = Re\left\{\int_0^a e^{iz}(-ie^{-iz})rdr\right\}, \tag{3.78}$$

or

$$\mathcal{E}_{inc} = Re\left\{\int_0^a rdr\right\}, \tag{3.79}$$

or

$$\mathcal{E}_{inc} = \frac{a^2}{2}. \tag{3.80}$$

Likewise to calculate the reflected power $\mathcal{E}_r$ in inlet, we use the reflected field

$$\phi_{ref} = \sum_{n=0}^{\infty} B_n R_{1n}(r) e^{-i\eta_n z}, \tag{3.81}$$

into (3.77), which gives

$$\mathcal{E}_r = -Re\Big[\int_0^a \sum_{m=0}^{\infty}\sum_{n=0}^{\infty} B_n B_m^* R_{1n} R_{1m}^* \eta_m^* e^{-i(\eta_n - \eta_m^*)z} r dr\Big]. \tag{3.82}$$

Note that, as $\tau_n, \quad n = 0, 1, 2\cdots$ are real which implies $R_{1m} = J_0(\tau_m r)$ to real, also $R_{1m}^* = R_{1m}$ and thus, (3.82) yields

$$\mathcal{E}_r = -Re\Big[\sum_{m=0}^{\infty}\sum_{n=0}^{\infty} B_n B_m^* \eta_m^* e^{-i(\eta_n - \eta_m^*)z} \int_0^a R_{1n} R_{1m} r dr\Big]. \tag{3.83}$$

On using orthogonality relation, (3.83) gives

$$\mathcal{E}_r = -Re\Big[\sum_{m=0}^{\infty}\sum_{n=0}^{\infty} B_n B_m^* \eta_m^* e^{-i(\eta_n - \eta_m^*)z} \delta_{mn} F_n\Big], \tag{3.84}$$

or

$$\mathcal{E}_r = -Re\Big[\sum_{n=0}^{\infty} |B_n|^2 \eta_m^* e^{-i(\eta_n - \eta_m^*)z} F_n\Big]. \tag{3.85}$$

As $\eta_n = \sqrt{1-\tau_n^2}$ is either real or pure imaginary. Therefore, (3.85), yields

$$\mathcal{E}_r = -Re\Big[\sum_{n=0}^{\infty} |B_n|^2 \eta_n F_n\Big]. \tag{3.86}$$

Likewise, for transmitted energy flux or power, we put

$$\phi_{tr} = \sum_{n=0}^{\infty} C_n R_{2n} e^{is_n z}, \tag{3.87}$$

(3.87) equation in (3.77) to get

$$\mathcal{E}_{tr} = -Re\Big[\int_0^b \sum_{m=0}^{\infty}\sum_{n=0}^{\infty} C_n C_m^* R_{2n} R_{2m}^* s_m^* e^{i(s_n - s_m^*)z} r dr\Big]. \tag{3.88}$$

Note that, as $\gamma_n, \quad n = 0, 1, 2\cdots$ are real which implies $R_{2m} = J_0(\gamma_m r)$ to real, also $R_{2m}^* = R_{2m}$ and thus, (3.88) yields

$$\mathcal{E}_{tr} = Re\Big[\sum_{m=0}^{\infty}\sum_{n=0}^{\infty} C_n C_m^* s_m^* e^{i(s_n - s_m^*)z} \int_0^b R_{2n} R_{2m} r dr\Big]. \tag{3.89}$$

On using orthogonality relation, (3.89) gives

$$\mathcal{E}_r = Re\Big[\sum_{m=0}^{\infty}\sum_{n=0}^{\infty} C_n C_m^* s_m^* e^{i(s_n - s_m^*)z} \delta_{mn} M_n\Big]. \tag{3.90}$$

As $s_n = \sqrt{1-\gamma_n^2}$ is either real or pure imaginary. Therefore, the above equation yields

$$\mathcal{E}_{tr} = Re\Big[\sum_{n=0}^{\infty} |C_n|^2 s_n M_n\Big]. \tag{3.91}$$

Now from conservation of energy law:

Energy flux in left hand side=Energy flux in right hand side,

$$\mathcal{E}_{inc} + \mathcal{E}_{ref} = \mathcal{E}_{tr}. \tag{3.92}$$

$$\frac{a^2}{2} - \sum_{n=0}^{\infty} |B_n|^2 \eta_n F_n = \sum_{n=0}^{\infty} |C_n|^2 s_n F_{2n}, \tag{3.93}$$

or

$$\frac{a^2}{2} = \sum_{n=0}^{\infty} |B_n|^2 \eta_n F_n + \sum_{n=0}^{\infty} |C_n|^2 s_n F_{2n}. \tag{3.94}$$

By dividing with $a^2/2$, we can scale incident energy to unity, that gives

$$1 = \frac{2}{a^2}\sum_{n=0}^{\infty} |B_n|^2 \eta_n F_n + \frac{2}{a^2}\sum_{n=0}^{\infty} |C_n|^2 s_n F_{2n}, \tag{3.95}$$

or

$$1 = \mathcal{E}_1 + \mathcal{E}_2, \tag{3.96}$$

where

$$\mathcal{E}_1 = \frac{2}{a^2} \sum_{n=0}^{\infty} |B_n|^2 \eta_n F_n, \tag{3.97}$$

and

$$\mathcal{E}_2 = \sum_{n=0}^{\infty} |C_n|^2 s_n F_{2n}, \tag{3.98}$$

are reflected and transmitted powers, respectively, when incident energy is unity. Note that (3.96) is known as power identity.

3.3.1 Numerical Solution

Here we truncate the system by taking m=n=0,1,2,...,N and The numerical calculations are carried out using the software MATHEMATICA, where the relevant parameters are set to specific values. These values are chosen from the [46] and are follows: frequency $f = 100Hz$, coupling parameter $\xi = 1Hz$, mass density of air $\rho = 1.2kgm^{-3}$, membrane mass density $\rho_m = 0.24kgm^{-3}$, sound speed in air $c = 343.5m/s$, $Z = i$ and tension $T = 124N$. In Fig. 3.2 to 3.10 the real and imaginary components are plotted against r are shown. It can be seen at the curve $\mathrm{Re}(\phi_{1z}(0,r))$ coincide to $\mathrm{Re}(\phi_{2z}(0,r))$ when $0 \leq r < a$. Likewise $\mathrm{Im}(\phi_{1z}(0,r))$ matches $\mathrm{Im}(\phi_{2z}(0,r))$. In Figs. 3.2 to 3.10, the matching conditions of problem-1 are shown with real and imaginary parts respectively by changing the values. In Figs. 3.2 and 3.10, the real and imaginary parts of normal velocity modes of region I and II are shown separately. In this way the truncated solution is verified numerically. To get the curves in Fig. 3.2 to 3.9 the radius of duct are kept at $\bar{a} = 0.55m, \bar{a} = 0.25m, \bar{a} = 0.10m, \bar{a} = 0.70m$, and length of duct are $\bar{L} = 0.25m, \bar{L} = 0.75m, \bar{L} = 0.60m, \bar{L} = 0.15m$, respectively where N = 10 terms.

While in Fig. 3.10 both real and imaginary parts are discussed combined by using the values in which the radius of duct is kept at $\bar{a} = 0.70m$, and the length of duct is $\bar{L} = 0.15m$.

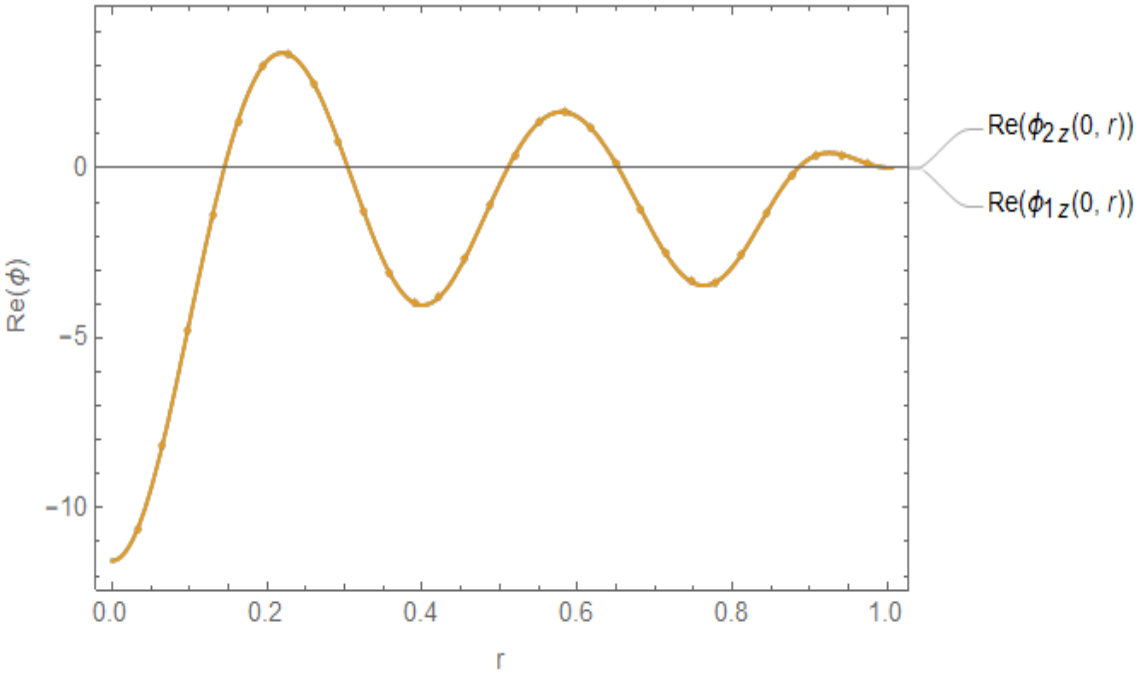

FIGURE 3.2: Real parts of velocities $\phi_{1z}(0, y)$ and $\phi_{2z}(0, y)$, plotted against r, where $\bar{a} = 0.55m$,and $N = 10$ terms

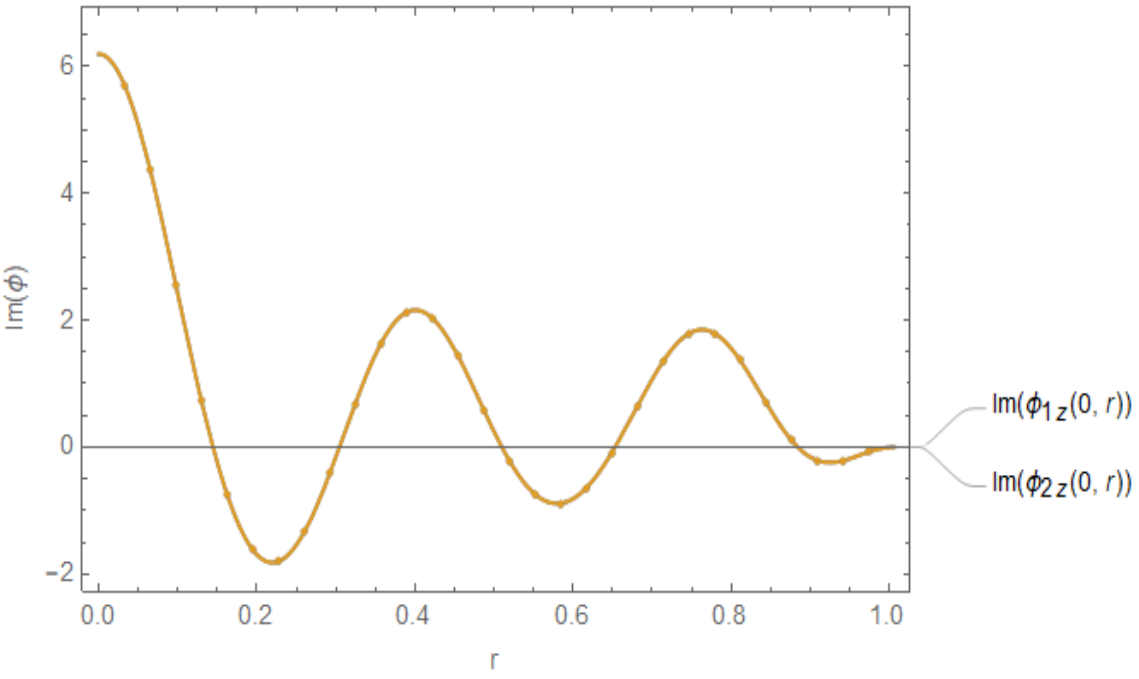

FIGURE 3.3: Imaginary parts of velocities $\phi_{1z}(0, y)$ and $\phi_{2z}(0, y)$, plotted against r, where $\bar{a} = 0.25m$,and $N = 10$ terms

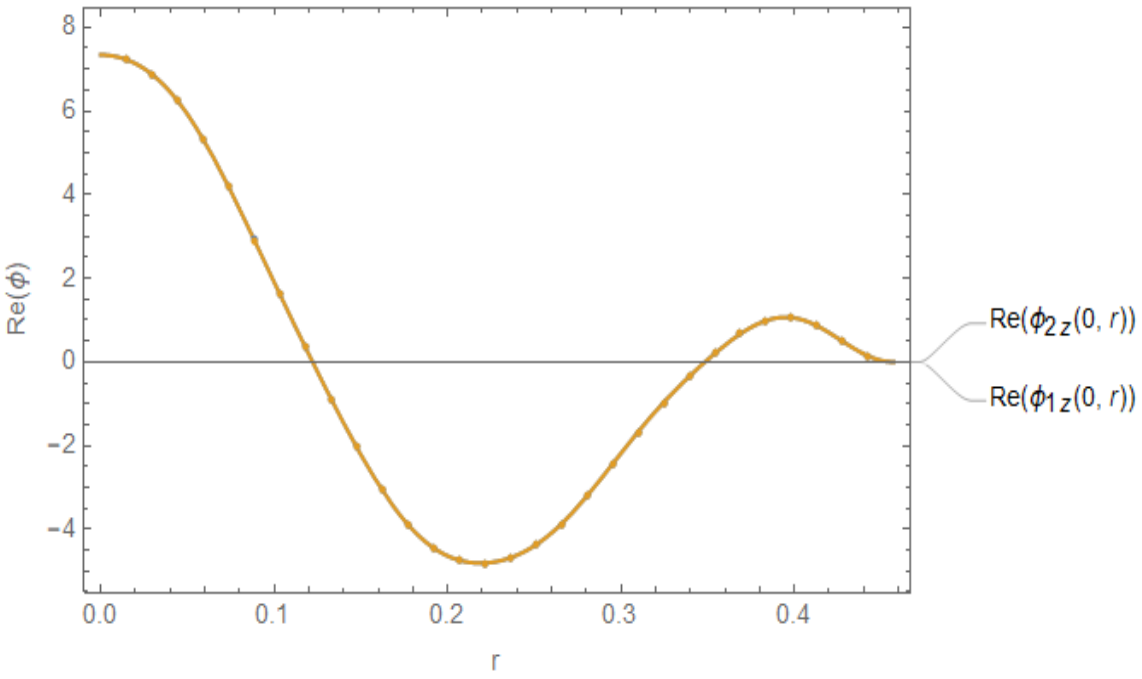

FIGURE 3.4: Real parts of velocities $\phi_{1z}(0, y)$ and $\phi_{2z}(0, y)$, plotted against r, where $\bar{a} = 0.10m$,and $N = 10$ terms

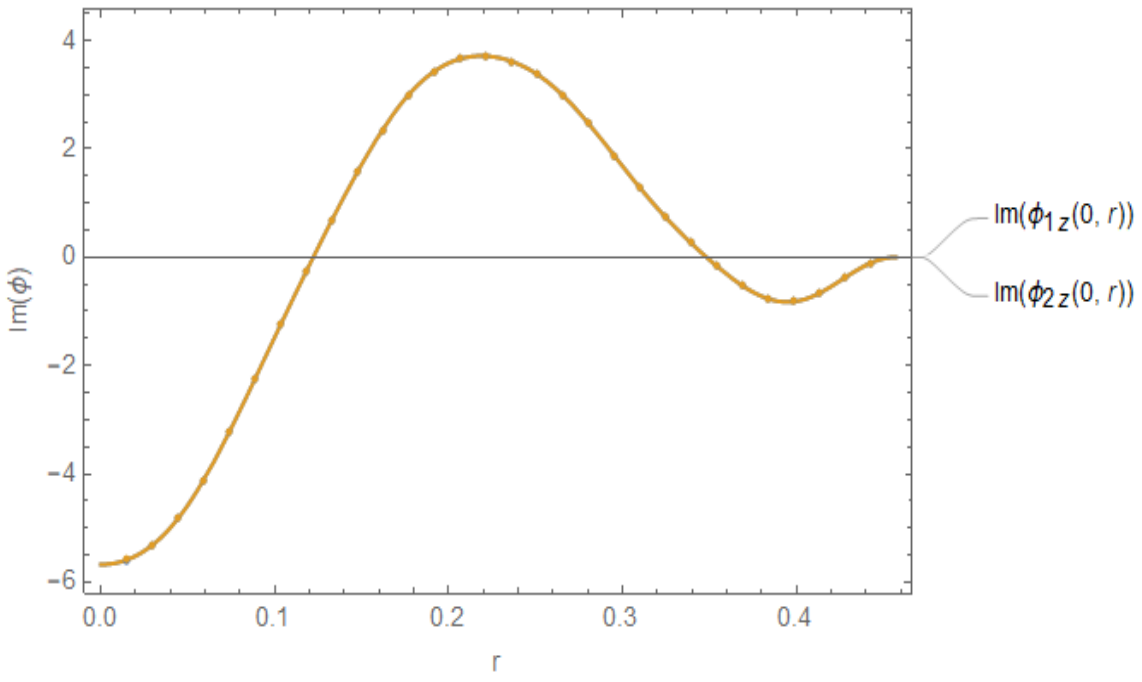

FIGURE 3.5: Imaginary parts of velocities $\phi_{1z}(0, y)$ and $\phi_{2z}(0, y)$, plotted against r, where$\bar{a} = 0.70m$,and $N = 10$ terms

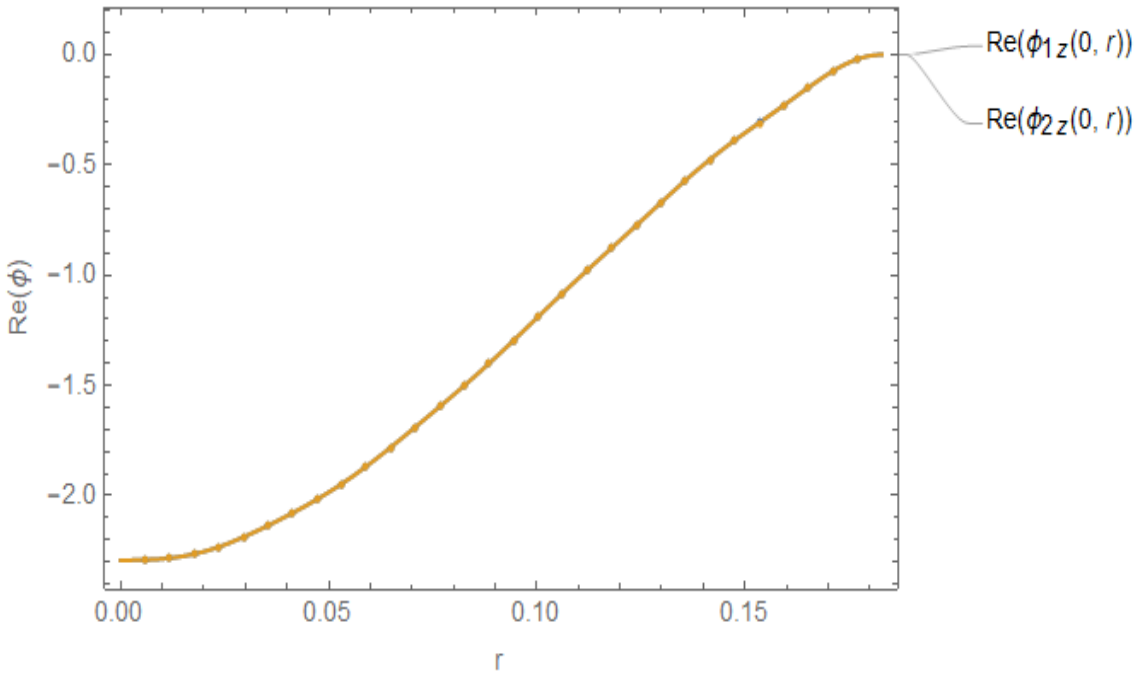

FIGURE 3.6: Real parts of velocities $\phi_{1z}(0, y)$ and $\phi_{2z}(0, y)$, plotted against r, where $N = 10$ terms

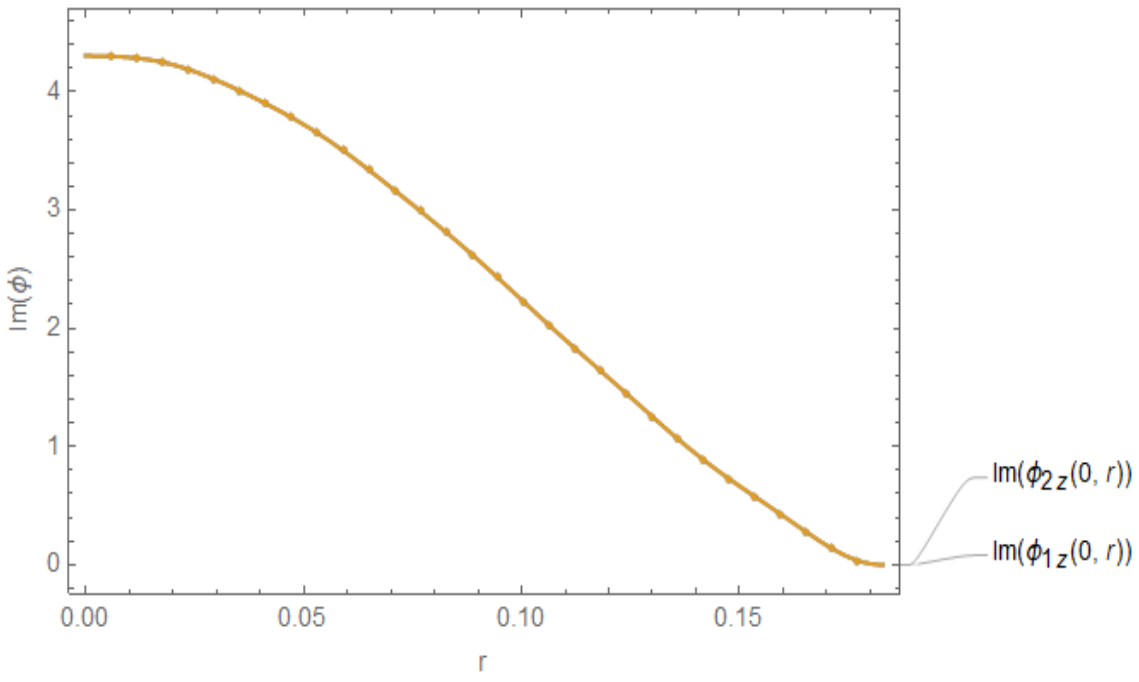

FIGURE 3.7: Imaginary parts of velocities $\phi_{1z}(0, y)$ and $\phi_{2z}(0, y)$, plotted against r, where $N = 10$ terms

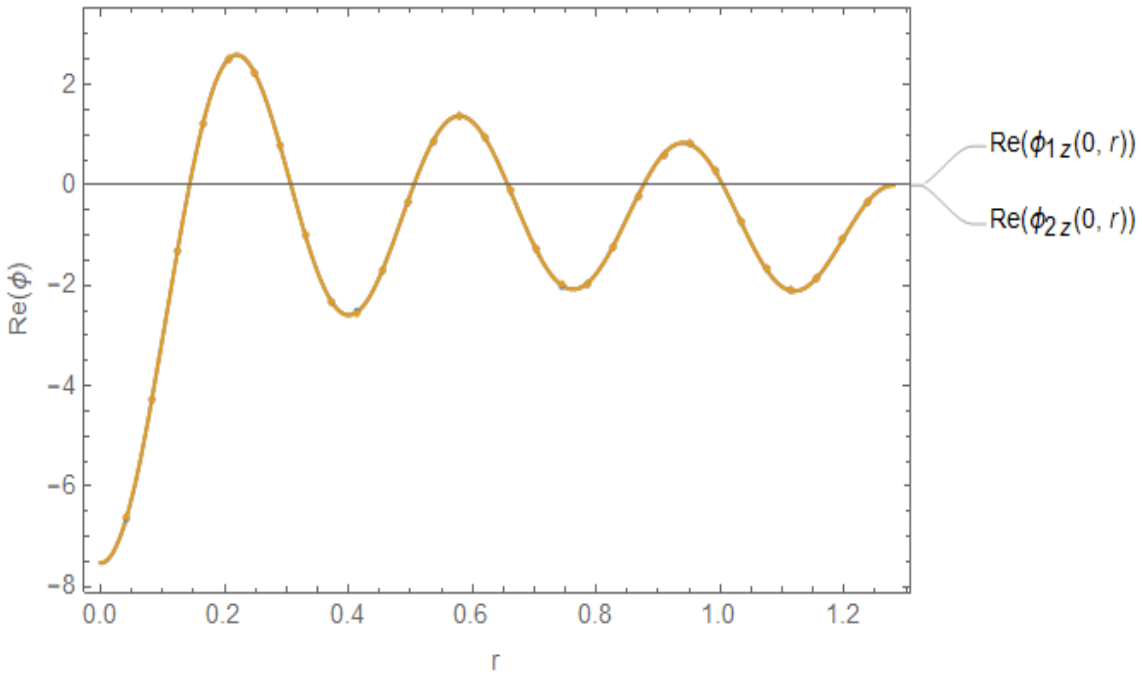

FIGURE 3.8: Real parts of velocities $\phi_{1z}(0, y)$ and $\phi_{2z}(0, y)$, plotted against r, where $N = 10$ terms

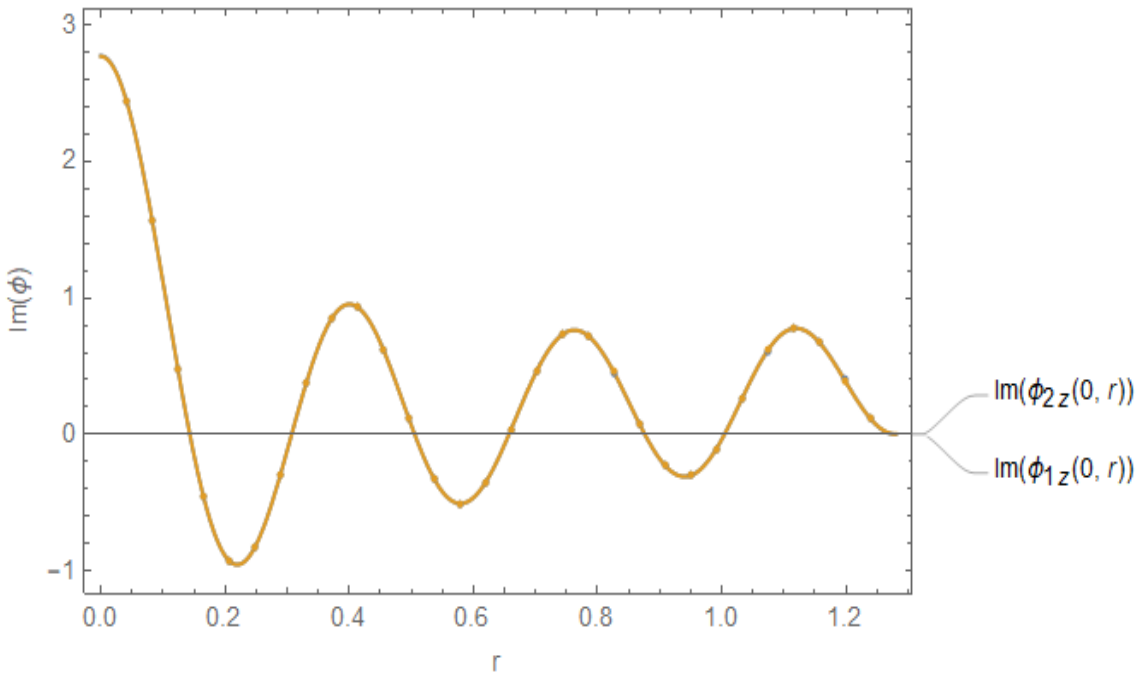

FIGURE 3.9: Imaginary parts of velocities $\phi_{1z}(0, y)$ and $\phi_{2z}(0, y)$, plotted against r, where $N = 10$ terms

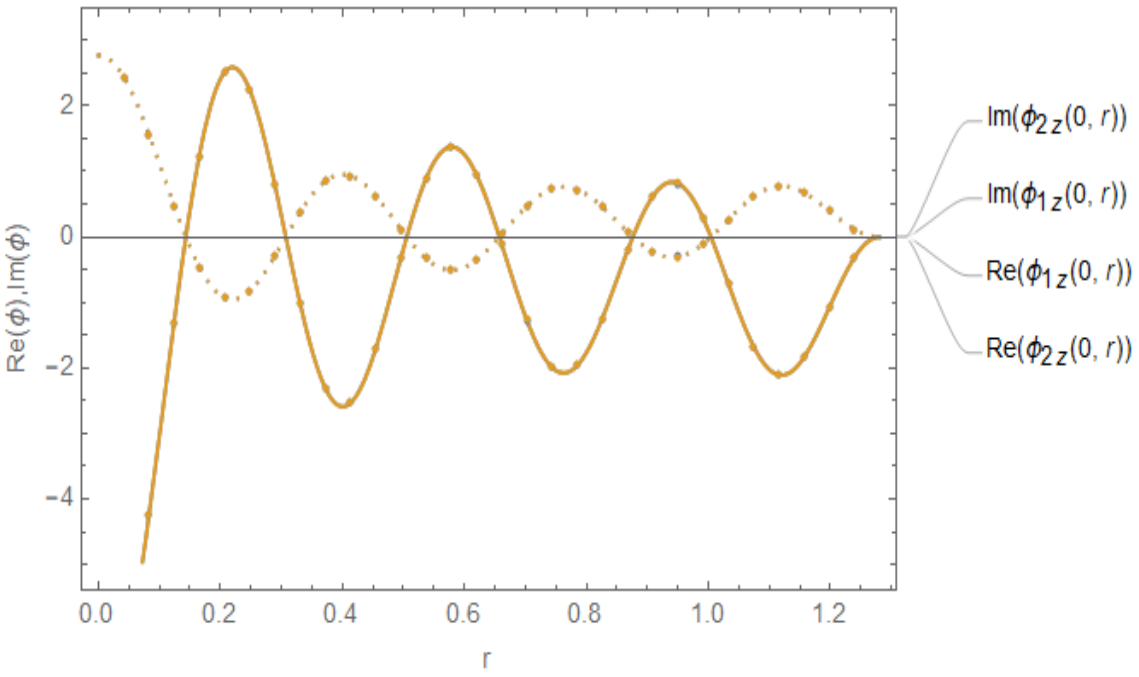

FIGURE 3.10: Real and imaginary parts of velocities $\phi_{1z}(0, y)$ and $\phi_{2z}(0, y)$, plotted against r, where $N = 10$ terms

The real and imaginary parts of normal velocities $\phi_{1x}(0, y)$ and $\phi_{2x}(0, y)$ for the respective regions are plotted in Figs. 3.2 to 3.10. It can be observed from figures that the velocities in fluid regions agree very well. It shows that the truncated terms of solution satisfy the matching conditions.

Furthermore, to see the satisfaction of power identity with truncated solution Figs. 3.11-3.12 are shown against frequency f. To get the curves in Figs. 3.11 and 3.12, we increase the radius of planar duct as $\bar{a} = 0.55m$ and $\bar{a} = 1m$, and $\bar{b} = 0.75m$, and $\bar{L} = 0.25m$, where N = 10 terms. Rest of the parameters are same as assumed to get the matching conditions graphs. In these graphs shown in Figs. 3.13 and 3.14, it can be seen that sum of reflected and transmitted remains unity as assumed in power identity against a. From 3.13-3.14, we can see that by changing frequency of duct as $f = 350Hz$ and $f = 750Hz$ a change in scattering powers may occurs.

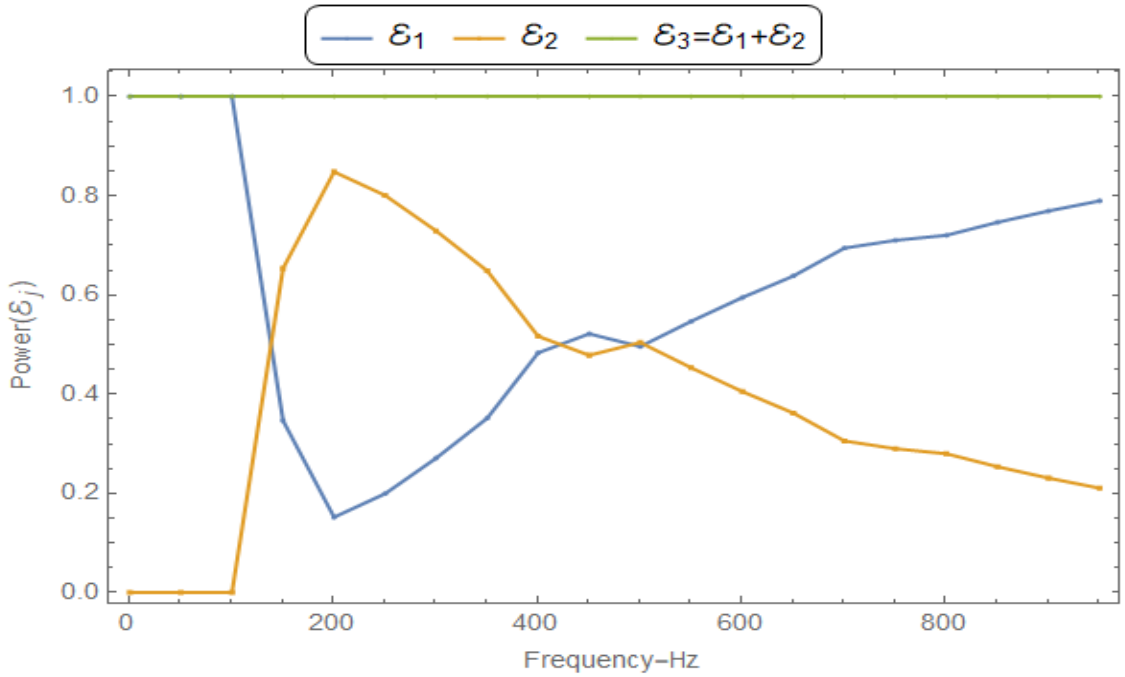

FIGURE 3.11: Scattering powers verses frequency when $\bar{a} = 0.55m$

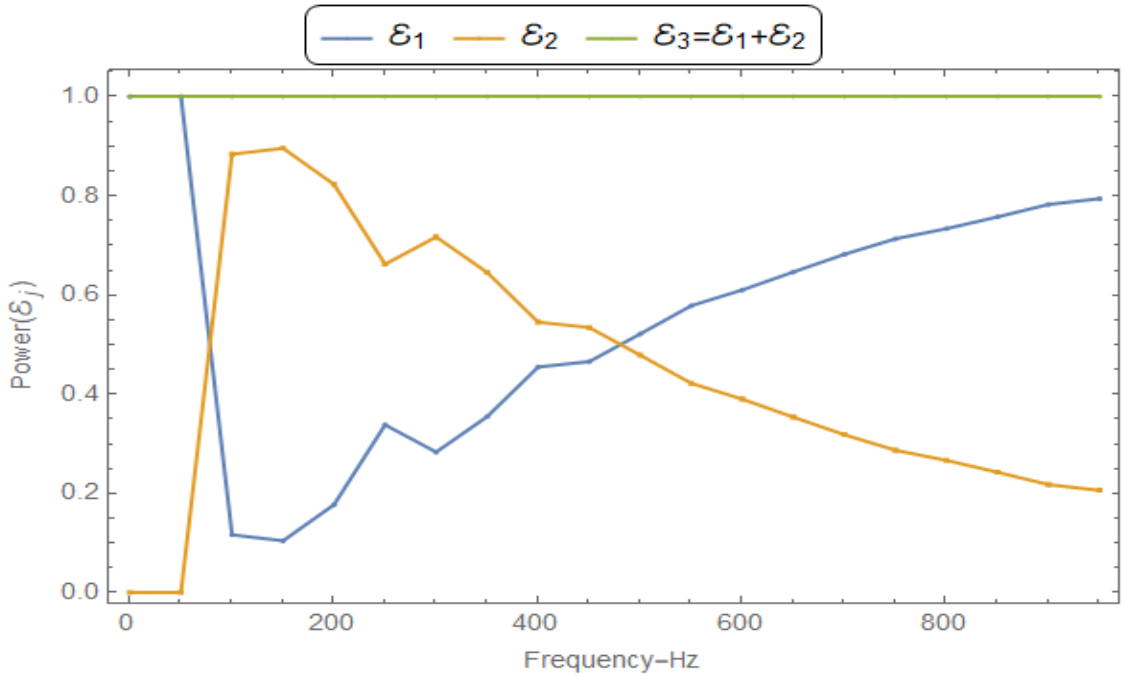

FIGURE 3.12: Scattering powers verses frequency when $\bar{a} = 1m$.

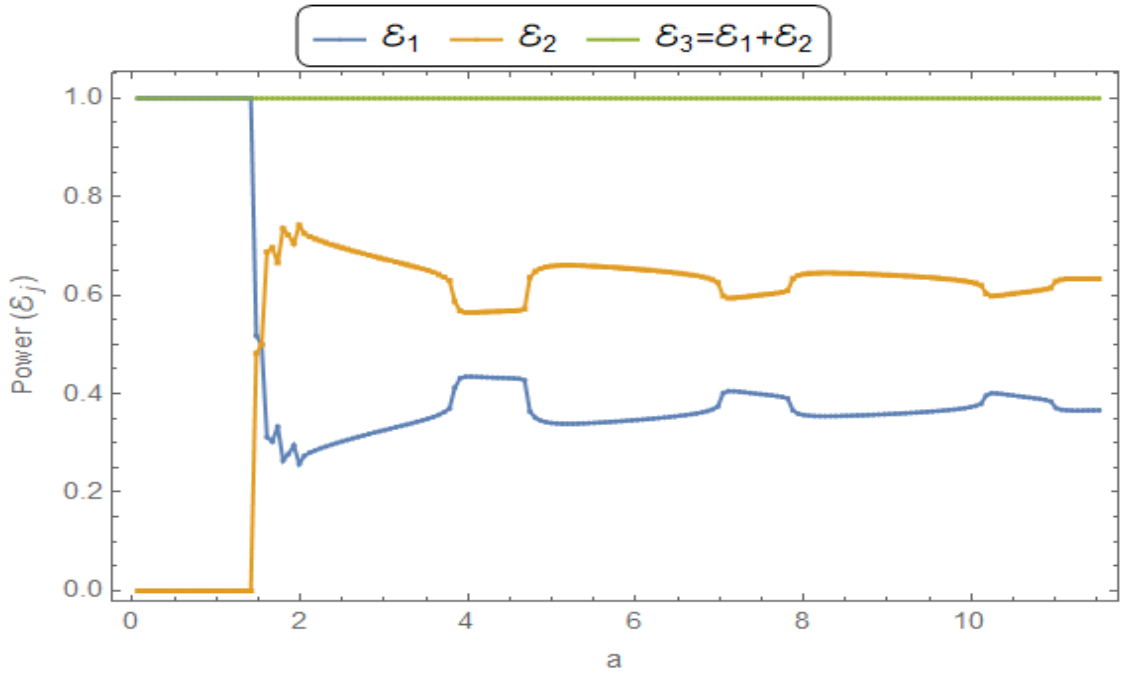

FIGURE 3.13: Scattering powers verses a when $f = 350Hz$

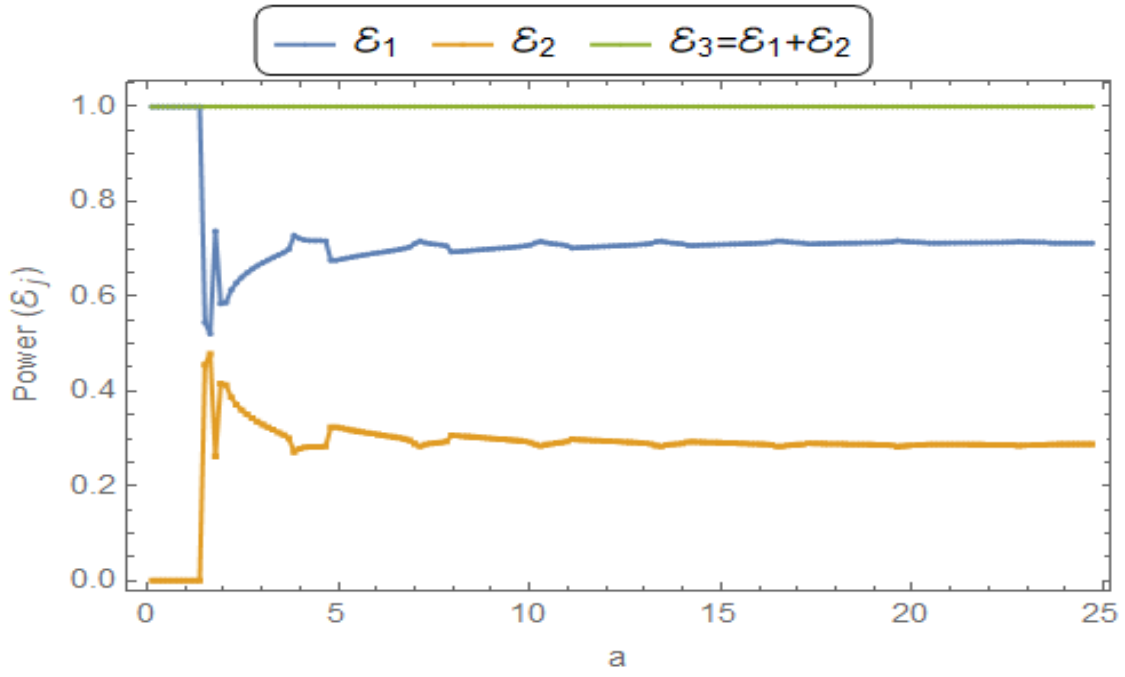

FIGURE 3.14: Scattering powers verses a when $f = 750Hz$

So from the figures 3.11-3.14 it is proved that, the sum of the scattering power propagation in different regions is unity which justifies the conserved power identity 3.96. In this way the confirmation of matching conditions and conserved power identity validation the truncated solution.

Chapter 4

The Propagation of Acoustic Waves from a Membrane Panel in a Waveguide Emitted by a Planar Piston

4.1 Introduction

This chapter explores the propagation and scattering of acoustic waves at interfaces consisting of rigid boundaries and membranes. Two specific problems are addressed:

- Problem 1: Micro-perforated elastic membrane with a planar piston in a cylindrical duct (Section 4.1)

- Problem 2: Scattering of piston radiation from a rigid cavity (Section 4.2)

The mathematical modeling of these problems is presented in Sections 4.1 and 4.2, respectively. The computational results and subsequent discussions are provided in Section 4.3.

4.2 Problem Formulation

The problem considered here may be radiated by the planar piston lying at $Z = 0$, along $0 < r < h$ and moving with dimensionless velocity U_0. The region at $h < r < a$ is considered to be rigid. For the sake of generality the planar mode exatations are also included. The elastic membrane lying at interface $Z = L$, while the region at $Z > L$ is assumed to contain lining along the $r = a$, which can be modelled by using mechanical impedance concept. However the region at $Z < L$ at $r = a$ is bounded by rigid wall condition. The physical configuration is shown in Fig. 4.1

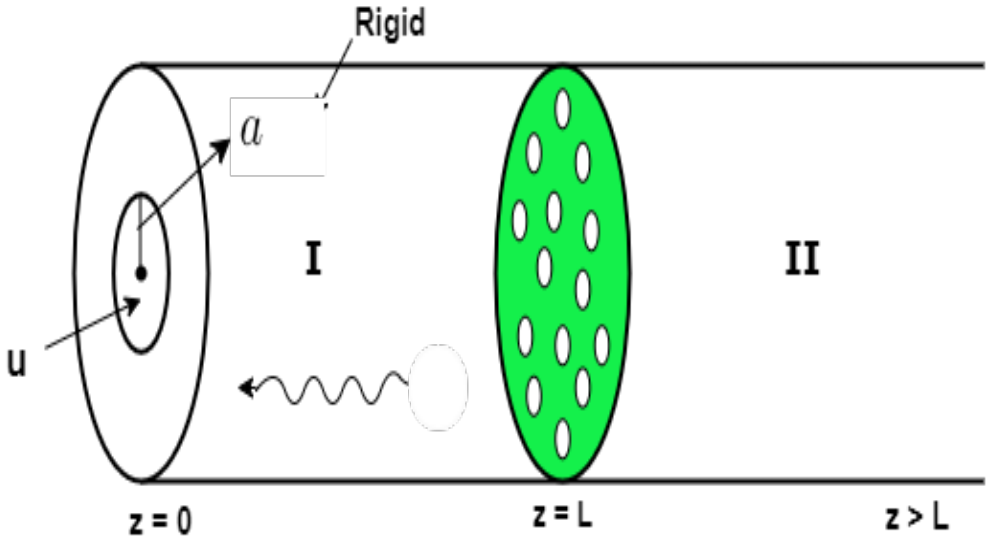

FIGURE 4.1: The physical configuration of waveguide

The governing boundary value problem includes, Helmholtz equation, rigid conditions, impedance conditions and membrane conditions. The problem is made dimensionless accordingly as explained in previous chapter. For region I, the non-dimensional Helmholtz equation and rigid boundary condition are

$$\left(\frac{\partial^2}{\partial r^2} + \frac{1}{r}\frac{\partial}{\partial r} + \frac{\partial^2}{\partial z^2} + 1\right)\phi_1(r, z) = 0, \tag{4.1}$$

and

$$\frac{\partial \phi_1}{\partial z}(a, z) = 0. \quad z < L \tag{4.2}$$

The exatation from planar piston at $z = 0$ can be defined as

$$\frac{\partial \phi_1}{\partial z}(r,0) = \begin{cases} U_0 & 0 \le r \le h, \\ 0 & h \le r \le a. \end{cases} \tag{4.3}$$

By solving (4.1) subject to (4.2) with separation of variable technique, for fundamental mode incident we can get eigenfunction expansion as

$$\phi_1(r,z) = \sum_{n=0}^{\infty} A_n R_{1n}(r) e^{i\eta_n z} + \sum_{n=0}^{\infty} B_n R_{1n}(r) e^{-i\eta_n z}, \tag{4.4}$$

where, $\eta_n = \sqrt{1-\tau_n^2}$ is n^{th} mode wavenumber propagating in region I having amplitude B_n, in which eigenvalues τ_n are roots of

$$J_0'(\tau_n(a) = 0,$$

the corresponding eigenfunctions $R_{1n}(r)$ satisfy orthogonality relation

$$\int_0^a R_{1m}(r) R_{1n} r dr = \delta_{mn} F_n.$$

For region II, the dimensionless fluid potential $\phi_2(r,z)$ satisfies the following Helmholtz equation and boundary condition

$$\left\{ \frac{\partial^2}{\partial r^2} + \frac{1}{r}\frac{\partial}{\partial r} + \frac{\partial^2}{\partial z^2} + 1 \right\} \phi_2(r,z) = 0. \quad z > L, \quad 0 < r < a \tag{4.5}$$

and

$$\phi_2 - i\mathcal{Z}\frac{\partial \phi_2}{\partial r} = 0. \quad r = a, \quad z \ge 0. \tag{4.6}$$

By solving (4.5) subject to (4.6) with separation of variable technique, for fundamental mode incident we can get eigenfunction expansion as:

$$\phi_2(r,z) = \sum_{n=0}^{\infty} D_n R_{2n} e^{is_n(z-L)}, \tag{4.7}$$

where $\{C_n, D_n\}$ are amplitudes of reflected and transmitted modes are unknowns. The quantity $s_n = \sqrt{1-\gamma_n^2}$ represents n^{th} mode wavenumber propagating in

region II and the eigenvalues γ_n are roots of

$$R_{2n}(r) = J_0(\gamma_n r); \quad \nu_n = \sqrt{1-\gamma_n^2}. \tag{4.8}$$

The corresponding eigenfunctions $R_{2n}(r)$ satisfy orthogonality relation

$$J_0(\gamma_n a) - i\mathcal{Z}J_0'(\gamma_n a) = 0. \tag{4.9}$$

Note that in aforementioned eigenfunction expansions in (4.4) and (4.7) are $\{A_n, B_n, D_n\}$ which are unknowns that will be found through mode-matching technique. Now using (4.1) into (4.3) we get

$$i\sum_{n=0}^{\infty} A_n\eta_n R_{1n} - i\sum_{n=0}^{\infty} B_n\eta_n R_{1n} = \begin{cases} U_0, \\ 0. \end{cases} \tag{4.10}$$

Multiply (4.10) by rR_{1m} and integrate 0 to a, we get

$$i\sum_{n=0}^{\infty}[A_n - B_n]\eta_n \int_0^a R_{1n}R_{1m}rdr = U_0\int_0^h R_{1m}rdr, \tag{4.11}$$

on using orthogonality relation (3.57), we get

$$A_m - B_m = \frac{U_0 Q_m}{i\eta_m F_m}, \tag{4.12}$$

simplification leads to

$$A_m = \frac{U_0 Q_m}{i\eta_m F_m} + B_m, \tag{4.13}$$

where

$$Q_m = \int_0^h R_{1m}rdr.$$

Now we use the membrane condition at $z = L$, to determine unknowns B_n and D_n, we rewrite (3.59) as follows:

$$\left(\frac{\partial^2}{\partial r^2} + \frac{1}{r}\frac{\partial}{\partial r} + \mu_m^2\right)\frac{\partial\phi_1}{\partial z} = \alpha_m(\phi_2 - \phi_1) + \frac{\delta(r-a)}{r}E_1, \tag{4.14}$$

where

$$\alpha_m = \frac{\rho c^2}{Tk}, \quad \mu_m = \frac{c^2}{c_m^2} \quad \text{and} \quad c_m = \sqrt{\frac{T}{\rho_m}}.$$

Now using (4.4) and (4.7) into (4.14), we get

$$\begin{aligned}
&i\sum_{n=0}^{\infty} A_n\eta_n R_{1n}''(r)e^{i\eta_n L} - i\sum_{n=0}^{\infty} B_n\eta_n R_{1n}''(r)e^{-i\eta_n L} + i\sum_{n=0}^{\infty} A_n\eta_n \frac{1}{r}R_n'(r)e^{i\eta_n L} \\
&- i\sum_{n=0}^{\infty} B_n\eta_n \frac{1}{r}R_n'(r)e^{-i\eta_n L} + \mu_m^2(i\sum_{n=0}^{\infty} A_n\eta_n R_{1n}(r)e^{i\eta_n L} - i\sum_{n=0}^{\infty} B_n\eta_n R_{1n}(r)e^{-i\eta_n L}) \\
&+ \alpha_m(\sum_{n=0}^{\infty} A_n R_{1n}(r)e^{i\eta_n L} + \sum_{n=0}^{\infty} B_n R_{1n}(r)e^{-i\eta_n L}) \\
&= \alpha_m \sum_{n=0}^{\infty} D_n R_{2n}(r) + \frac{\delta(r-a)}{r}E_1,
\end{aligned} \tag{4.15}$$

which on simplification leads to

$$\sum_{n=0}^{\infty} A_n\Delta_{1n}R_{1n}(r) + \sum_{n=0}^{\infty} B_n\Delta_{2n}R_{1n}(r) = \alpha_m \sum_{n=0}^{\infty} D_n R_{2n}(r) + \frac{\delta(r-a)}{r}E_1. \tag{4.16}$$

where

$$\Delta_{1n} = \left(i\eta_n(-{\tau_n}^2 + {\mu_m}^2) + \alpha_m\right)e^{i\eta_n L},$$

and

$$\Delta_{2n} = \left(-i\eta_n(-{\tau_n}^2 + {\mu_m}^2) + \alpha_m\right)e^{-i\eta_n L}.$$

Multiplying (4.46) with $rR_{1m}(r)$ and integrating $0 \le r \le a$, we get

$$\begin{aligned}
&\sum_{n=0}^{\infty} A_n\Delta_{1n}\int_0^a R_{1m}R_{1n}rdr + \sum_{n=0}^{\infty} B_n\Delta_{2n}\int_0^a R_{1m}R_{1n}rdr \\
&= \alpha_m \sum_{n=0}^{\infty} D_n\int_0^a R_{1m}R_{2n}rdr + E_1\int_0^a \frac{\delta(r-a)}{r}R_{1m}(r)rdr.
\end{aligned} \tag{4.17}$$

On using orthogonality relation (3.57), we found

$$\sum_{n=0}^{\infty} A_n\Delta_{1n}\delta_{mn}F_n + \sum_{n=0}^{\infty} B_n\Delta_{2n}\delta_{mn}F_n = \alpha_m \sum_{n=0}^{\infty} D_n P_{mn} + E_1 R_{1m}(a), \tag{4.18}$$

which on simplification leads to

$$B_m = -\frac{A_m \Delta_{1m}}{\Delta_{2m}} + \frac{\alpha_m}{\Delta_{2m} F_m} \sum_{n=0}^{\infty} D_n P_{mn} + \frac{E_1 R_{1m}(a)}{F_m \Delta_{2m}}. \tag{4.19}$$

Now using (4.13) and (4.19), we get the value of A_m and B_m in term of D_m

$$A_m = \Delta_{3m} \left(\frac{U_0 Q_m}{i\eta_m F_m} + \frac{\alpha_m}{\Delta_{2m} F_m} \sum_{n=0}^{\infty} D_n P_{mn} + \frac{E_1 R_{1m}(a)}{F_m \Delta_{2m}} \right), \tag{4.20}$$

and

$$B_m = \Delta_{3m} \left(\frac{-U_0 Q_m \Delta_{1m}}{i\eta_m F_m \Delta_{2m}} + \frac{\alpha_m}{\Delta_{2m} F_m} \sum_{n=0}^{\infty} D_n P_{mn} + \frac{E_1 R_{1m}(a)}{F_m \Delta_{2m}} \right), \tag{4.21}$$

where

$$\Delta_{3m} = \frac{\Delta_{2m}}{\Delta_{2m} + \Delta_{1m}}.$$

Here, constant E_1 is unknown and it will be found through some condition on rim at $r = a$. For sake of generality, we consider spring like condition (3.18), which on using $w = \frac{\partial \phi_1}{\partial z}$ becomes

$$\frac{\partial^2 \phi_1}{\partial r \partial z} + \xi \frac{\partial \phi_1}{\partial z} = 0. \tag{4.22}$$

On using (4.4) into (4.22), we get

$$\sum_{n=0}^{\infty} (A_n e^{i\eta_n L} - B_n e^{-i\eta_n L}) \eta_n \left(R'_{1n}(a) + \xi R_{1n}(a) \right) = 0. \tag{4.23}$$

From (4.20) and (4.21), we have

$$A_n = \Delta_{3n} \left(\frac{U_0 Q_n}{i\eta_n F_n} + \frac{\alpha_n}{\Delta_{2n} F_n} \sum_{p=0}^{\infty} D_p P_{np} + \frac{E_1 R_{1n}(a)}{F_n \Delta_{2n}} \right), \tag{4.24}$$

and

$$B_n = \Delta_{3n} \left(\frac{-U_0 Q_n \Delta_{1n}}{i\eta_n F_n \Delta_{2n}} + \frac{\alpha_n}{\Delta_{2n} F_n} \sum_{p=0}^{\infty} D_p P_{np} + \frac{E_1 R_{1n}(a)}{F_n \Delta_{2n}} \right), \tag{4.25}$$

Using (4.24) and (4.25) into (4.23), we find values of constant E_1 as:

$$\begin{aligned}
&\sum_{n=0}^{\infty}\Delta_{3n}\left(\frac{U_0Q_n}{i\eta_nF_n}+\frac{\alpha_n}{\Delta_{2n}F_n}\sum_{p=0}^{\infty}D_pP_{np}+\frac{E_1R_{1n}(a)}{F_n\Delta_{2n}}\right)e^{i\eta_nL}\\
&(\eta_nR'_{1n}(a)+\xi\eta_nR_{1n}(a))=0\\
&-\Delta_{3n}\left(\frac{-U_0Q_n\Delta_{1n}}{i\eta_nF_n\Delta_{2n}}+\frac{\alpha_n}{\Delta_{2n}F_n}\sum_{p=0}^{\infty}D_pP_{np}+\frac{E_1R_{1n}(a)}{F_n\Delta_{2n}}\right)e^{-i\eta_nL}\\
&(\eta_nR'_{1n}(a)+\xi\eta_nR_{1n}(a))=0,
\end{aligned}\tag{4.26}$$

which on simplification leads to

$$E_1=-\frac{N}{S}-\frac{\alpha}{S}\sum_{n=0}^{\infty}\sum_{P=0}^{\infty}\frac{2i\Delta_{3n}D_pP_{mp}\sin(\eta_nL)\eta_n(R'_{1n}(a)+\xi R_{1n}(a))}{F_n\Delta_{2n}},\tag{4.27}$$

where

$$S=\sum_{n=0}^{\infty}\frac{2i\sin(\eta_nL)\Delta_{3n}\eta_nR_{1n}(R'_{1n}(a)+\xi R_{1n}(a))}{F_n\Delta_{2n}},\tag{4.28}$$

and

$$N=\sum_{n=0}^{\infty}\Delta_{3n}\left(\frac{U_0Q_n}{i\eta_nF_n}e^{i\eta_nL}+\frac{U_0Q_n\Delta_{1n}}{i\eta_nF_n\Delta_{2n}}e^{-i\eta_nL}\right)(\eta_nR'_{1n}(a)+\xi\eta_nR_{1n}(a)).$$

Now on using (4.4) and (4.7), equation (3.20) becomes

$$\sum_{n=0}^{\infty}D_ns_nR_{2n}(r)=\sum_{n=0}^{\infty}A_n\eta_nR_{1n}(r)e^{i\eta_nL}-\sum_{n=1}^{\infty}B_n\eta_nR_{1n}(r)e^{-i\eta_nL}.\tag{4.29}$$

Multiplying by rR_{2m} and integrating from 0 to a with (4.26), we get

$$\begin{aligned}
&\sum_{n=0}^{\infty}D_ns_n\int_0^aR_{2m}R_{2n}rdr=\sum_{n=0}^{\infty}A_n\eta_ne^{i\eta_nL}\int_0^aR_{2m}R_{1n}rdr\\
&-\sum_{n=0}^{\infty}B_n\eta_ne^{-i\eta_nL}\int_0^aR_{2m}R_{1n}rdr,
\end{aligned}\tag{4.30}$$

on using orthogonality relation (4.10), we get

$$D_m=\frac{1}{s_mF_{2m}}\left(\sum_{n=0}^{\infty}\eta_n(A_ne^{i\eta_nL}-B_ne^{-i\eta_nL})P_{nm}\right),\tag{4.31}$$

4.3 Scattering of Piston Radiation from Rigid Cavity

The problem considered in this section, is formed by taking the membrane at interfaces. Note that all the boundaries of the waveguide are rigid and inside of the waveguide is filled with compressible fluid. The geometrical configuration is shown in Fig. 4.2.

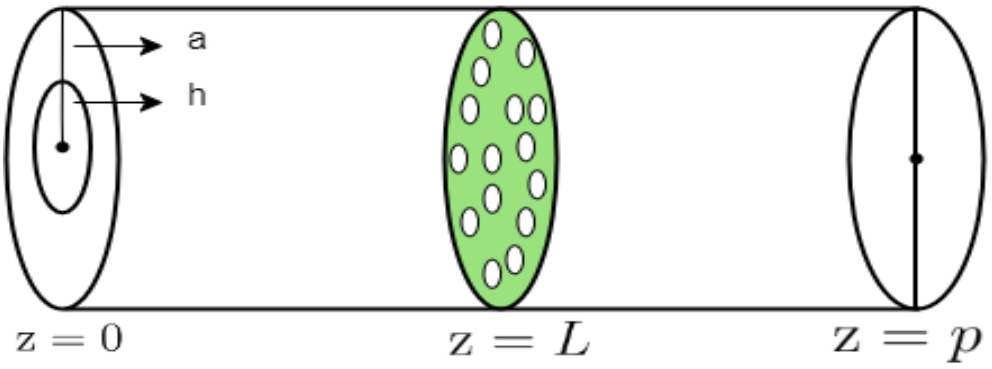

FIGURE 4.2: The physical configuration of waveguide

The governing boundary value problem includes, Helmholtz equation, rigid conditions and membrane conditions. The problem is made dimensionless accordingly as explained in previous sections. For region I, the non-dimensional Helmholtz equation and rigid boundary condition are

$$\left(\frac{\partial^2}{\partial r^2}+\frac{1}{r}\frac{\partial}{\partial r}+\frac{\partial^2}{\partial z^2}+1\right)\phi_1(r,z)=0, \tag{4.32}$$

and

$$\frac{\partial \phi_1}{\partial z}(r,0)=\begin{cases} U_0 & 0\le r\le h, \\ 0 & h\le r\le a. \end{cases} \tag{4.33}$$

By solving (4.32) subject to (4.33) with separation of variable technique, for fundamental mode incident we can get eigenfunction expansion as:

$$\phi_1(r,z)=\sum_{n=0}^{\infty}A_nR_{1n}(r)e^{i\eta_n z}+\sum_{n=0}^{\infty}B_nR_{1n}(r)e^{-i\eta_n z}, \tag{4.34}$$

where, $\eta_n = \sqrt{1-\tau_n^2}$ is n^{th} mode wavenumber propagating in region I having amplitudes $\{A_n, B_n\}$, in which eigenvalues τ_n are roots of

$$J_0'(\tau_n a) = 0. \tag{4.35}$$

The corresponding eigenfunctions $R_{1n}(r)$ satisfy orthogonality relation

$$\int_0^a R_{1m}(r)R_{1n}rdr = \delta_{mn}F_n. \tag{4.36}$$

For region II, the non-dimensional Helmholtz equation and rigid boundary condition are

$$\left\{\frac{\partial^2}{\partial r^2} + \frac{1}{r}\frac{\partial}{\partial r} + \frac{\partial^2}{\partial z^2} + 1\right\}\phi_2(r,z) = 0, \tag{4.37}$$

and

$$\frac{\partial \phi_2}{\partial z}(r,p) = 0. \tag{4.38}$$

By solving (4.37) subject to (4.38) with separation of variable technique, for fundamental mode incident we can get eigenfunction expansion as:

$$\phi_2(r,z) = \sum_{n=0}^{\infty} C_n R_{2n}(r)e^{-is_n(z-L)} + \sum_{n=0}^{\infty} D_n R_{2n}e^{is_n(z+L)}, \tag{4.39}$$

where, $\{C_n, D_n\}$ is amplitude of reflected and transmitted modes is unknown. The quantity $s_n = \sqrt{1-\gamma_n^2}$ represents n^{th} mode wavenumber propagating in region II and the eigenvalues γ_n are roots of

$$J_0(\gamma_n a) - i\mathcal{Z}J_0'(\gamma_n a) = 0. \tag{4.40}$$

The corresponding eigenfunctions $R_{2n}(r)$ satisfy orthogonality relation

$$\int_0^b R_{2m}(r)R_{2n}rdr = \delta_{mn}F_{2n}. \tag{4.41}$$

Note that in aforementioned eigenfunction expansions in (4.34) and (4.39) are $\{A_n, B_n, C_n, D_n\}$ which are unknowns that will be found through mode-matching

technique. Now using (4.38) into (4.39), we get

$$C_n e^{-is_n(P-L)} - D_n e^{is_n(P+L)} = 0, \tag{4.42}$$

which leads to

$$C_n = D_n e^{2is_nP}. \tag{4.43}$$

Now using (4.33) into (4.34), we get

$$i\sum_{n=0}^{\infty} A_n\eta_n R_{1n} - i\sum_{n=0}^{\infty} B_n\eta_n R_{1n} = \begin{cases} U_0, \\ 0. \end{cases} \tag{4.44}$$

Multiply (4.44) by rR_{1m} and integrate 0 to a, we found

$$i\sum_{n=0}^{\infty}[A_n - B_n]\eta_n \int_0^a R_{1n}R_{1m}rdr = U_0\int_0^h R_{1m}rdr, \tag{4.45}$$

which on simplification leads to

$$A_m - B_m = \frac{U_0Q_m}{i\eta_m F_m}, \tag{4.46}$$

which leads to

$$A_m = \frac{U_0Q_m}{i\eta_m F_m} + B_m, \tag{4.47}$$

where

$$Q_m = \int_0^h R_{1m}rdr.$$

Now we use the membrane condition at $z = L$, to determine unknowns B_n and C_n, we rewrite (3.59) as follows:

$$\left(\frac{\partial^2}{\partial r^2} + \frac{1}{r}\frac{\partial}{\partial r} + \mu_m^2\right)\frac{\partial\phi_1}{\partial z} = \alpha_m(\phi_2 - \phi_1) + \frac{\delta(r-a)}{r}E_1, \tag{4.48}$$

where

$$\alpha_m = \frac{\rho c^2}{Tk}, \quad \mu_m = \frac{c^2}{c_m^2} \quad \text{and} \quad c_m = \sqrt{\frac{T}{\rho_m}}.$$

Now using (4.34) and (4.39), we get

$$\begin{aligned}
&i\sum_{n=0}^{\infty} A_n\eta_n R_{1n}''(r)e^{i\eta_n L} - i\sum_{n=0}^{\infty} B_n\eta_n R_{1n}''(r)e^{-i\eta_n L} + i\sum_{n=0}^{\infty} A_n\eta_n\frac{1}{r}R_n'(r)e^{i\eta_n L}\\
&- i\sum_{n=0}^{\infty} B_n\eta_n\frac{1}{r}R_n'(r)e^{-i\eta_n L} + \mu_m^2(i\sum_{n=0}^{\infty} A_n\eta_n R_{1n}(r)e^{i\eta_n L} - i\sum_{n=0}^{\infty} B_n\eta_n R_{1n}(r)e^{-i\eta_n L})\\
&+ \alpha_m(\sum_{n=0}^{\infty} A_n R_{1n}(r)e^{i\eta_n L} + \sum_{n=0}^{\infty} B_n R_{1n}(r)e^{-i\eta_n L})\\
&= \alpha_m\left(\sum_{n=0}^{\infty} C_n R_{2n}(r)e^{-is_n(P-L)} + \sum_{n=0}^{\infty} D_n R_{2n}(r)e^{is_n(P+L)}\right) + \frac{\delta(r-a)}{r}E_1,
\end{aligned} \tag{4.49}$$

which on simplification leads to

$$\begin{aligned}
&\sum_{n=0}^{\infty} A_n\Delta_{1n}R_{1n}(r) + \sum_{n=0}^{\infty} B_n\Delta_{2n}R_{1n}(r)\\
&= \alpha_m\left(\sum_{n=0}^{\infty} C_n R_{2n}(r)e^{-is_n(P-L)} + \sum_{n=0}^{\infty} D_n R_{2n}(r)e^{is_n(P+L)}\right) + \frac{\delta(r-a)}{r}E_1,
\end{aligned} \tag{4.50}$$

where

$$\Delta_{1n} = \left(i\eta_n(-{\tau_n}^2 + {\mu_m}^2) + \alpha_m\right)e^{i\eta_n L},$$

and

$$\Delta_{2n} = \left(-i\eta_n(-{\tau_n}^2 + {\mu_m}^2) + \alpha_m\right)e^{-i\eta_n L}.$$

Multiplying (4.47) with rR_{1m} and integrating $0 \le r \le a$, we get

$$\begin{aligned}
&\sum_{n=0}^{\infty} A_n\Delta_{1n}\int_0^a R_{1m}R_{1n}rdr + \sum_{n=0}^{\infty} B_n\Delta_{2n}\int_0^a R_{1m}R_{1n}rdr\\
&= \alpha_m\left(\sum_{n=0}^{\infty} C_n e^{-is_n(P-L)} + \sum_{n=0}^{\infty} D_n e^{is_n(P+L)}\right)\int_0^a R_{1m}R_{2n}rdr\\
&+ E_1\int_0^a \frac{\delta(r-a)}{r}R_{1m}(r)rdr.
\end{aligned} \tag{4.51}$$

on using orthogonality relation (3.53), we have

$$\begin{aligned}&\sum_{n=0}^{\infty} A_n\Delta_n\delta_{mn}F_n + \sum_{n=0}^{\infty} B_n\Delta_n\delta_{mn}F_n\\&= \alpha_m \sum_{n=0}^{\infty}\left(C_n e^{-is_n(P-L)} + D_n e^{is_n(P+L)}\right) P_{mn} + E_1 R_{1m}(a),\end{aligned} \tag{4.52}$$

making some mathematical rearrangements we found that

$$\begin{aligned}B_m = \frac{-A_m\Delta_{1m}}{\Delta_{2m}} + \frac{\alpha_m}{\Delta_{2m}F_m}\sum_{n=0}^{\infty}\left(C_n e^{-is_n(P-L)} + D_n e^{is_n(P+L)}\right) P_{mn}\\ + \frac{E_1 R_{1m}(a)}{F_m\Delta_{2m}}.\end{aligned} \tag{4.53}$$

Now using (4.47) and (4.53), we get the value of A_m and B_m in term of D_m

$$\begin{aligned}A_m = \Delta_{3m}\frac{U_0 Q_m}{i\eta_m F_m} + \Delta_{3m}\frac{\alpha_m}{\Delta_{2m}F_m}\sum_{n=0}^{\infty}\left(C_n e^{-is_n(P-L)} + D_n e^{is_n(P+L)}\right) P_{mn}\\ + \Delta_{3m}\frac{E_1 R_{1m}(a)}{F_m\Delta_{2m}},\end{aligned} \tag{4.54}$$

and

$$\begin{aligned}B_m = \Delta_{3m}\frac{-U_0 Q_m\Delta_{1m}}{i\eta_m F_m\Delta_{2m}} + \Delta_{3m}\frac{\alpha_m}{\Delta_{2m}F_m}\sum_{n=0}^{\infty}\left(C_n e^{-is_n(P-L)} + D_n e^{is_n(P+L)}\right) P_{mn}\\ + \Delta_{3m}\frac{E_1 R_{1m}(a)}{F_m\Delta_{2m}},\end{aligned} \tag{4.55}$$

where

$$\Delta_{3m} = \frac{\Delta_{2m}}{\Delta_{2m} + \Delta_{1m}}.$$

Here, constant E_1 is unknown and it will be found through some condition on rim at $r = a$. For sake of generality, we consider spring like condition (3.18), which on using $w = \frac{\partial\phi_1}{\partial z}$ becomes,

$$\frac{\partial^2\phi_1}{\partial r\partial z} + \xi\frac{\partial\phi_1}{\partial z} = 0. \tag{4.56}$$

On using (4.34) into (4.56), we get

$$\sum_{n=0}^{\infty}(A_n e^{i\eta_n L} - B_n e^{-i\eta_n L})\eta_n \left(R'_{1n}(a) + \xi R_{1n}(a)\right) = 0. \tag{4.57}$$

From (4.54) and (4.55), we have

$$\begin{aligned} A_n = \Delta_{3n}\frac{U_0 Q_n}{i\eta_n F_n} + \Delta_{3n}\frac{\alpha_n}{\Delta_{2n}F_n}\sum_{p=0}^{\infty}\left(C_p e^{-is_p(P-L)} + D_p e^{is_p(P+L)}\right)P_{np} \\ + \Delta_{3n}\frac{E_1 R_{1n}(a)}{F_n\Delta_{2n}}, \end{aligned} \tag{4.58}$$

and

$$\begin{aligned} B_n = \Delta_{3n}\frac{-U_0 Q_n\Delta_{1n}}{i\eta_n F_n\Delta_{2n}} + \Delta_{3n}\frac{\alpha_n}{\Delta_{2n}F_n}\sum_{p=0}^{\infty}\left(C_p e^{-is_p(P-L)} + D_p e^{is_p(P+L)}\right)P_{np} \\ + \Delta_{3n}\frac{E_1 R_{1n}(a)}{F_n\Delta_{2n}}. \end{aligned} \tag{4.59}$$

Using (4.58) and (4.59) into (4.57), we find values of constant E_1 as:

$$\begin{aligned} &\sum_{n=0}^{\infty}\Delta_{3n}\left(\frac{U_0 Q_n}{i\eta_n F_n} + \frac{\alpha_n}{\Delta_{2n}F_n}\sum_{p=0}^{\infty}(C_p e^{-is_p(P-L)} + D_p e^{is_p(P+L)})P_{np} + \frac{E_1 R_{1n}(a)}{F_n\Delta_{2n}}\right)e^{i\eta_n L} \\ &- \Delta_{3n}\left(\frac{-U_0 Q_n\Delta_{1n}}{i\eta_n F_n\Delta_{2n}} + \frac{\alpha_n}{\Delta_{2n}F_n}\sum_{p=0}^{\infty}(C_p e^{-is_p(P-L)} + D_p e^{is_p(P+L)})P_{np} + \frac{E_1 R_{1n}(a)}{F_n\Delta_{2n}}\right) \\ &e^{-i\eta_n L}\left(\eta_n R'_{1n}(a) + \xi\eta_n R_{1n}(a)\right) = 0, \end{aligned} \tag{4.60}$$

which on simplification leads to

$$\begin{aligned} E_1 = -\frac{N}{S} - \frac{\alpha}{S}\sum_{n=0}^{\infty}\sum_{P=0}^{\infty}\frac{2i\Delta_{3n}(C_p e^{-is_p(P-L)} + D_p e^{is_p(P+L)})P_{mp}\sin(\eta_n L)\eta_n}{F_n\Delta_{2n}} \\ \frac{(R'_{1n}(a) + \xi R_{1n}(a))}{F_n\Delta_{2n}}, \end{aligned} \tag{4.61}$$

where

$$S = \sum_{n=0}^{\infty}\frac{2i\sin(\eta_n L)\Delta_{3n}\eta_n R_{1n}(R'_{1n}(a) + \xi R_{1n}(a))}{F_n\Delta_{2n}}, \tag{4.62}$$

and

$$N=\sum_{n=0}^{\infty}\Delta_{3n}\left(\frac{U_0Q_n}{i\eta_nF_n}e^{i\eta_nL}+\frac{U_0Q_n\Delta_{1n}}{i\eta_nF_n\Delta_{2n}}e^{-i\eta_nL}\right)(\eta_nR'_{1n}(a)+\xi\eta_nR_{1n}(a))\,.$$

Now on using (4.34) and (4.39), equation (3.20) becomes

$$\begin{aligned}&\sum_{n=0}^{\infty}C_ns_nR_{2n}(r)e^{-is_n(P-L)}-\sum_{n=0}^{\infty}D_ns_nR_{2n}(r)e^{is_n(P+L)}=\sum_{n=0}^{\infty}A_n\eta_nR_{1n}(r)e^{i\eta_nL}\\&-\sum_{n=1}^{\infty}B_n\eta_nR_{1n}(r)e^{-i\eta_nL}.\end{aligned}\tag{4.63}$$

Multiplying by rR_{2m} and integrating from 0 to a with (4.63), we get

$$\begin{aligned}&\sum_{n=0}^{\infty}C_ns_ne^{-is_n(P-L)}\int_0^aR_{2m}R_{2n}rdr-\sum_{n=0}^{\infty}D_ns_ne^{is_n(P+L)}\int_0^aR_{2m}R_{2n}rdr\\&=\sum_{n=0}^{\infty}A_n\eta_ne^{i\eta_nL}\int_0^aR_{2m}R_{1n}rdr-\sum_{n=0}^{\infty}B_n\eta_ne^{-i\eta_nL}\int_0^aR_{2m}R_{1n}rdr,\end{aligned}\tag{4.64}$$

on using orthogonality relation (4.10), we get

$$D_m=-C_ne^{-2is_nL}+\frac{1}{s_mF_{2m}e^{is_n(P+L)}}\left(\sum_{n=0}^{\infty}\eta_n(A_ne^{i\eta_nL}-B_ne^{-i\eta_nL})P_{nm}\right).\tag{4.65}$$

Now using (4.43) and (4.65), we get the value of C_m and D_m in term of A_m and B_m

$$C_m=\frac{e^{2is_nP}}{s_mF_{2m}(1+e^{2is_n(P-L)})}\left(\sum_{n=0}^{\infty}\eta_n(A_ne^{i\eta_nL}-B_ne^{-i\eta_nL})P_{nm}\right),\tag{4.66}$$

and

$$D_m=\frac{1}{s_mF_{2m}(1+e^{2is_n(P-L)})}\left(\sum_{n=0}^{\infty}\eta_n(A_ne^{i\eta_nL}-B_ne^{-i\eta_nL})P_{nm}\right).\tag{4.67}$$

4.4 Numerical Solution

Here we truncate the system by taking m=n=0,1,2,...,N and The numerical calculations are carried out using the software MATHEMATICA, where the relevant parameters are set to specific values. These values are chosen from the [ref of numerical values] and are follows: frequency $f = 100Hz$, coupling parameter $\xi = 1Hz$, mass density of air $\rho = 1.2kgm^{-3}$, membrane mass density $\rho_m = 0.24kgm^{-3}$, sound speed in air $c = 343.5m/s$, $Z = i$ and tension $T = 125N$. In Fig. 4.3 to 4.8 the real and imaginary components are plotted against r are shown. It can be seen at the curve $\mathrm{Re}(\phi_{1z}(0,r))$ coincide to $\mathrm{Re}(\phi_{2z}(0,r))$ when $0 \leq r < a$. Likewise $\mathrm{Im}(\phi_{1z}(0,r))$ matches $\mathrm{Im}(\phi_{2z}(0,r))$.

In Figs. 4.3 to 4.8, the matching conditions of problem-1 are shown with real and imaginary parts respectively by changing the values. In Figs. 4.3 to 4.8, the real and imaginary parts of normal velocity modes of region I and II are shown separately. In this way the truncated solution is verified numerically. To get the curves in Fig. 4.3 to 4.8 the radius of duct is kept at $\bar{a} = 1m, \bar{a} = 0.55m, \bar{a} = 0.45m$, where $N = 5$ terms. While in Fig.4.9 both real and imaginary parts are discussed combined by using the values in which the radius of duct is kept at $\bar{a} = 1m$.

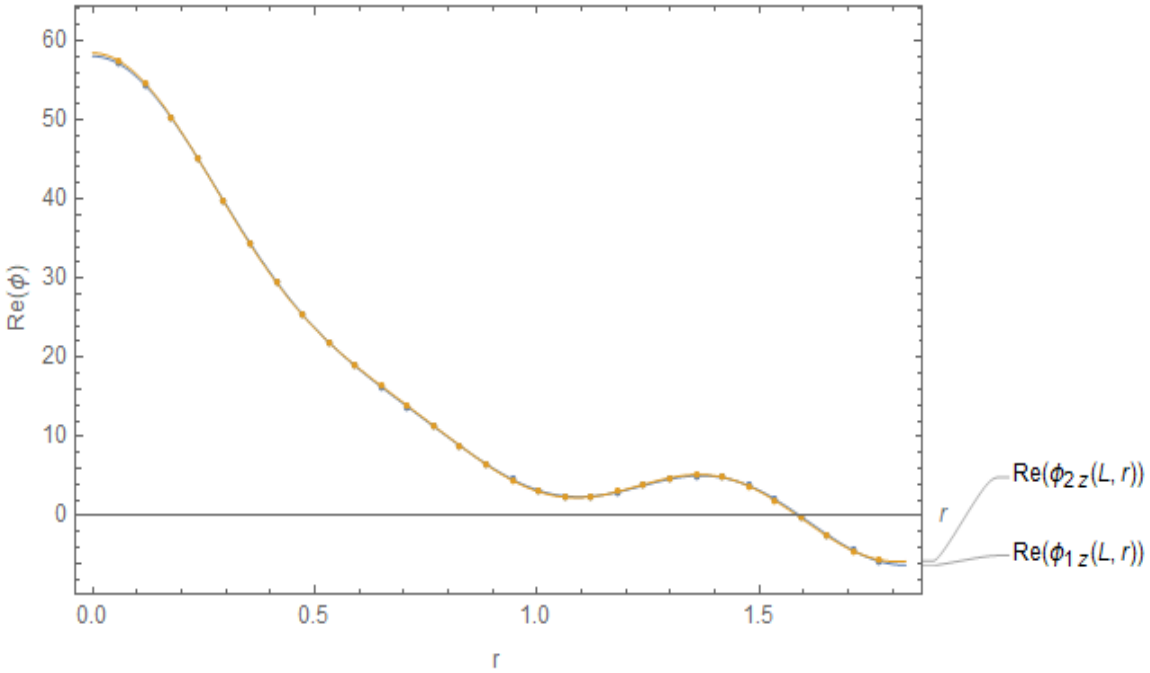

FIGURE 4.3: Real part of velocities $\phi_{1z}(0,y)$ and $\phi_{2z}(0,y)$, plotted against r, where $N = 10$ terms

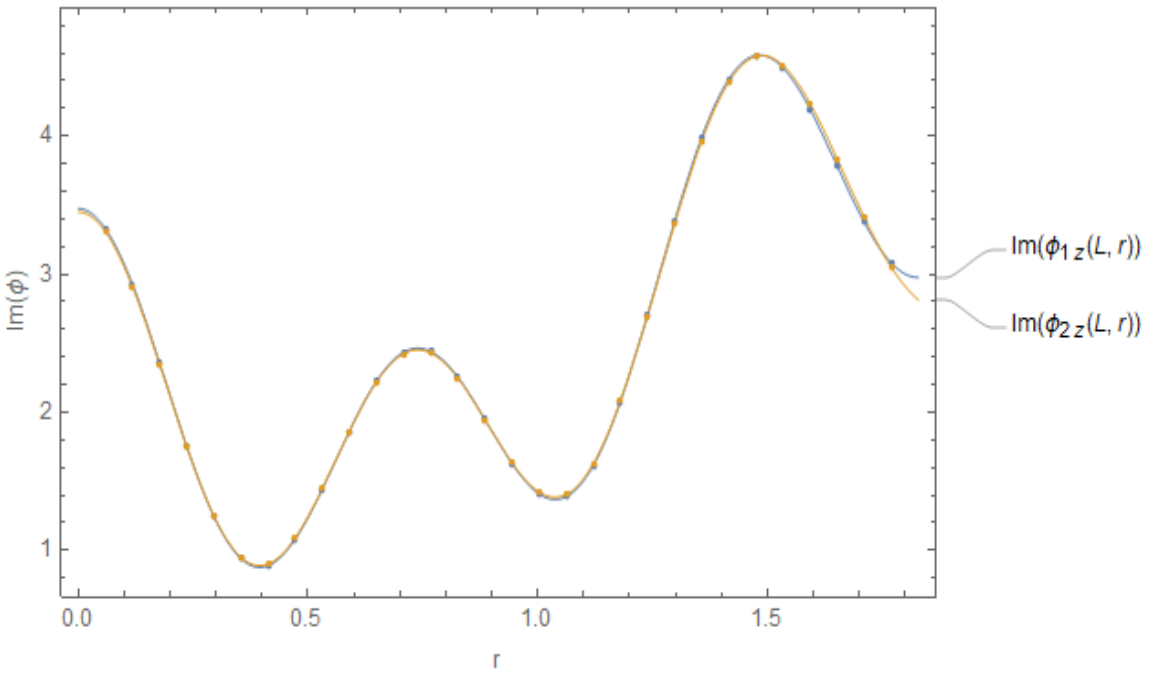

FIGURE 4.4: Imaginary part of velocities $\phi_{1z}(0, y)$ and $\phi_{2z}(0, y)$, plotted against r, where $N = 10$ terms

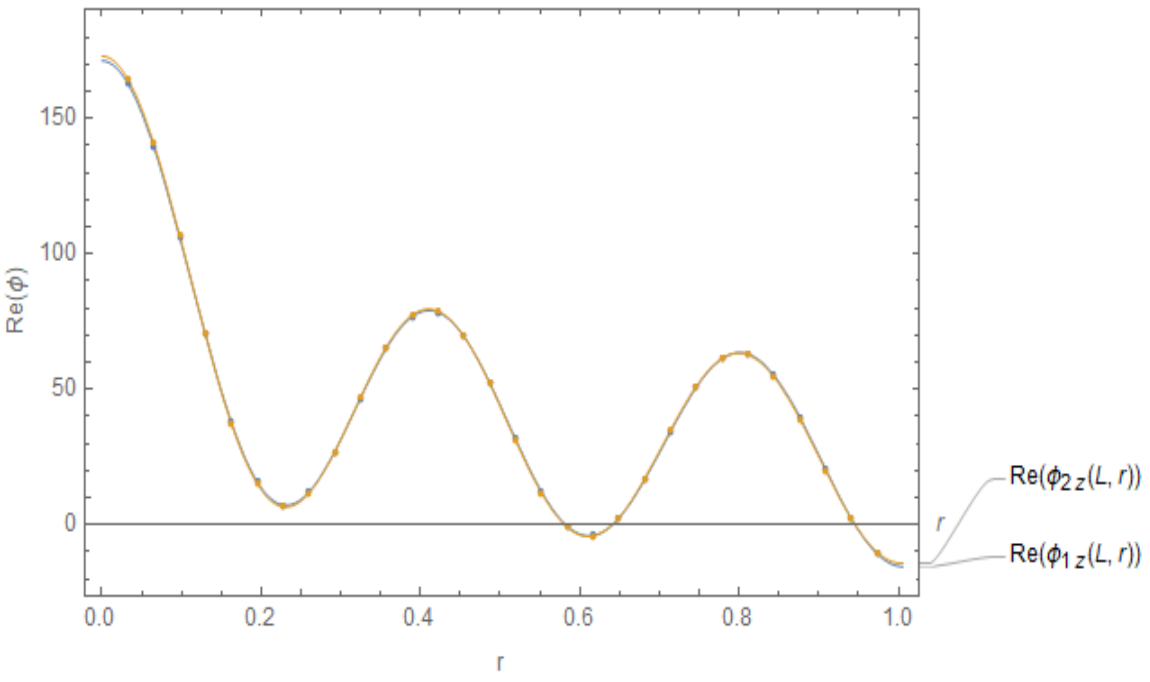

FIGURE 4.5: Real part of velocities $\phi_{1z}(0, y)$ and $\phi_{2z}(0, y)$, plotted against r, where $N = 5$ terms

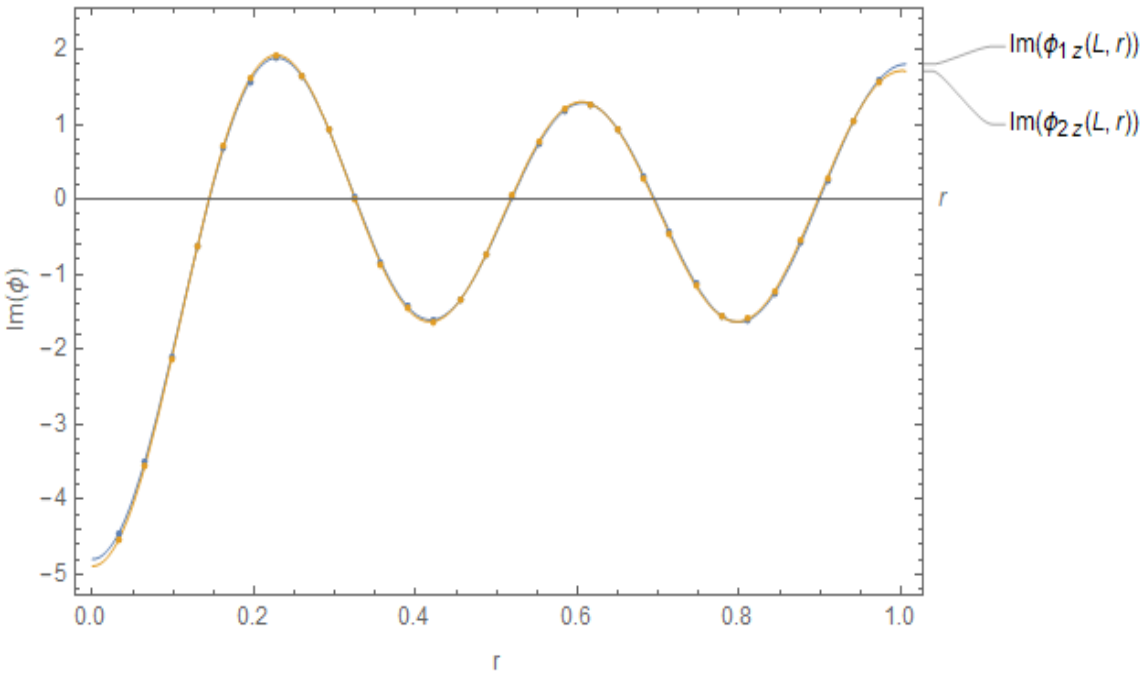

FIGURE 4.6: Imaginary part of velocities $\phi_{1z}(0, y)$ and $\phi_{2z}(0, y)$, plotted against r, where $N = 5$ terms

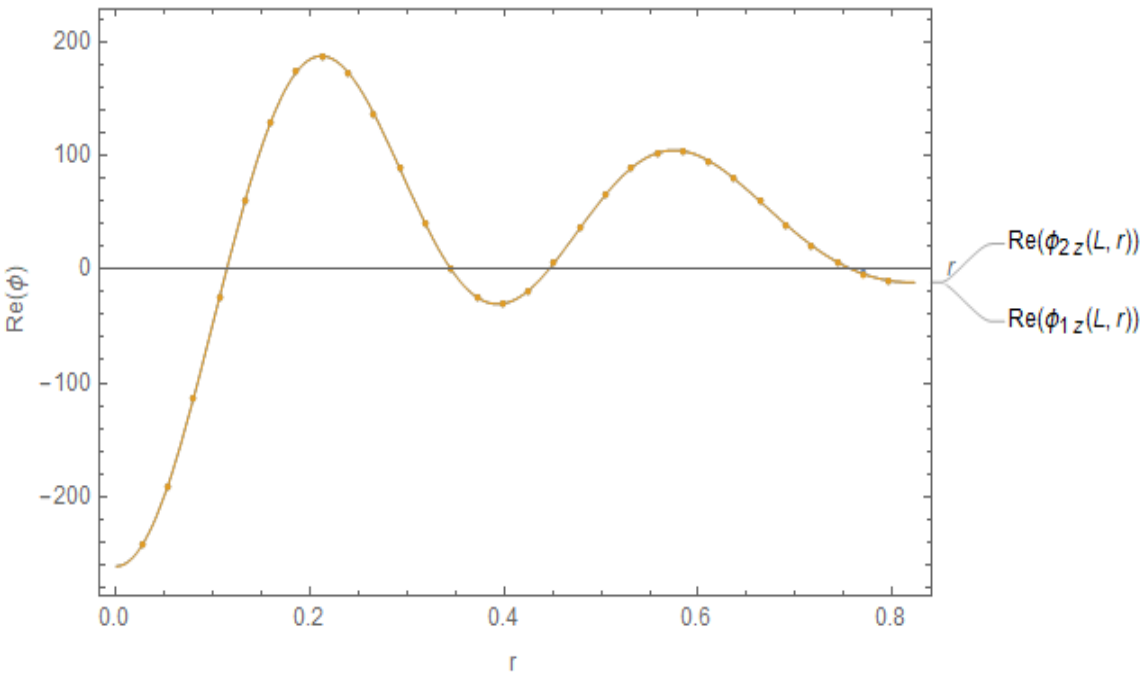

FIGURE 4.7: Real part of velocities $\phi_{1z}(0, y)$ and $\phi_{2z}(0, y)$, plotted against r, where $N = 15$ terms

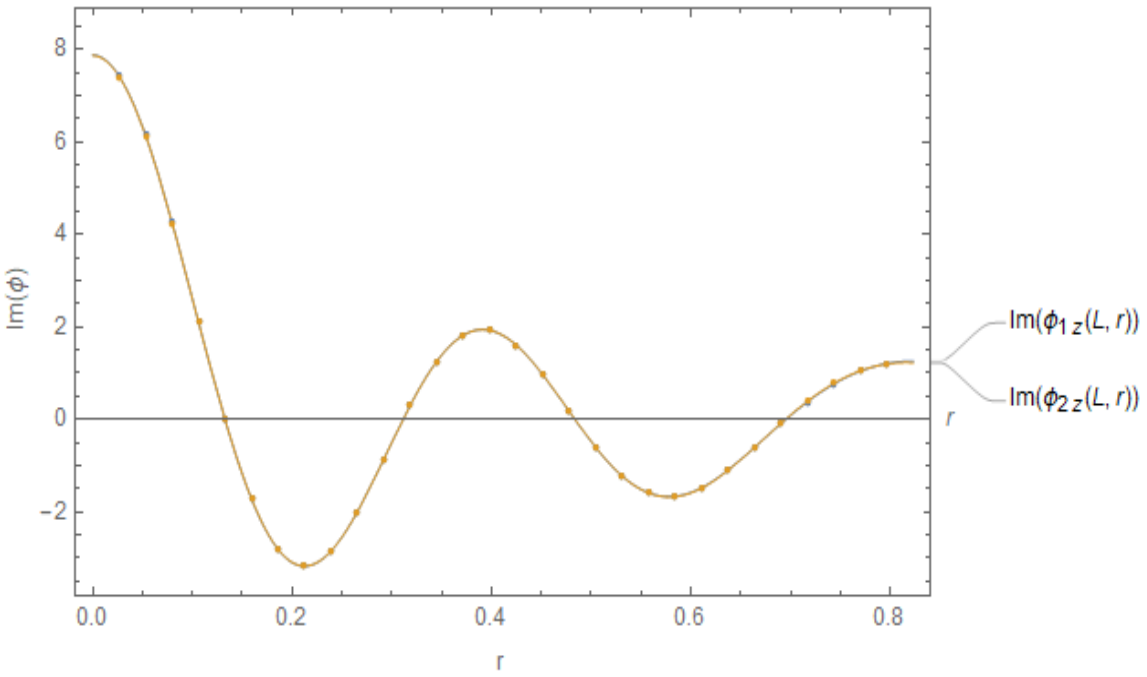

FIGURE 4.8: Imaginary part of velocities $\phi_{1z}(0, y)$ and $\phi_{2z}(0, y)$, plotted against r, where $N = 15$ terms

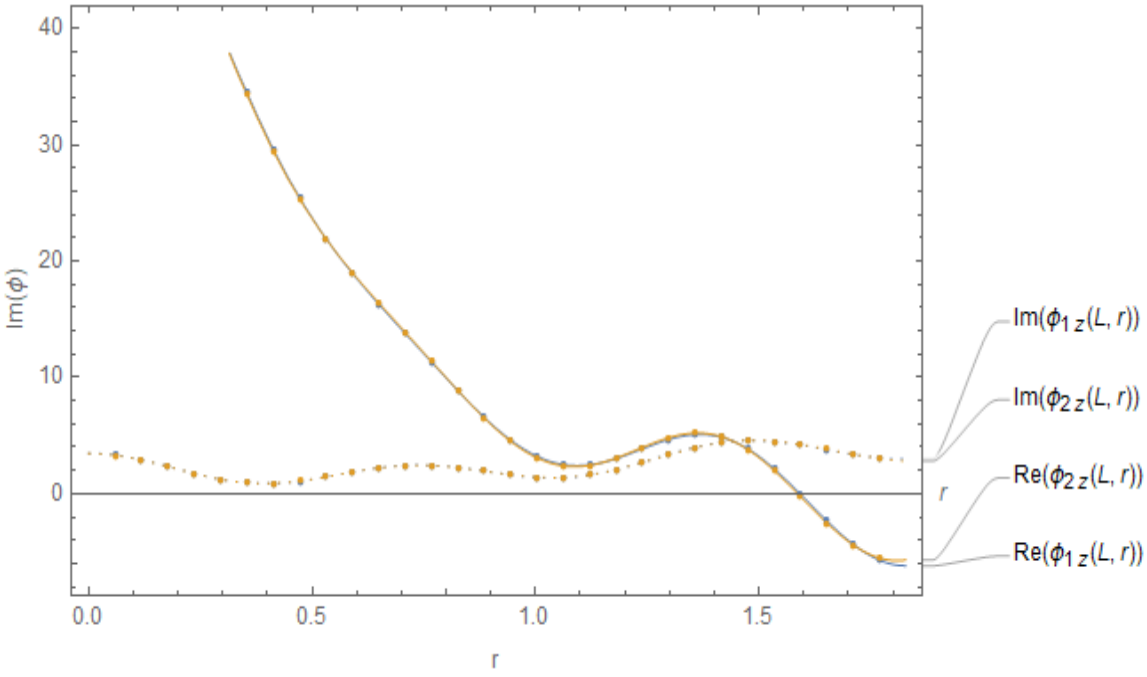

FIGURE 4.9: Real and Imaginary part of velocities $\phi_{1z}(0, y)$ and $\phi_{2z}(0, y)$, plotted against r, where $N = 15$ terms

The real and imaginary parts of normal velocities $\phi_{1x}(0, y)$ and $\phi_{2x}(0, y)$ for the respective regions are plotted in Figs. (4.3) to (4.9). It can be observed from figures that the velocities in fluid regions agree very well. It shows that the truncated

terms of solution satisfy the matching conditions. The impedance of piston in dimensional form can be expressed as [31]

$$\bar{\mathcal{C}} = \frac{\bar{\mathcal{F}}}{\bar{\mathcal{U}}}, \tag{4.68}$$

where $\bar{\mathcal{F}} = \frac{\bar{\mathcal{P}}}{A}$ is the dimensional force on the piston in which A denotes the piston area, that is $A = \pi(\bar{b}^2)$, and $\bar{\mathcal{U}}$ is the dimension velocity of the piston. This is related to dimensional velocity U_0 as $\bar{\mathcal{U}} = U_0 c$. The dimensional pressure $\bar{p}$ of the piston is

$$\bar{p} = \int_0^b \bar{p}(\bar{r}, 0)\bar{r}d\bar{r}, \tag{4.69}$$

where $\bar{p} = i\omega\rho\bar{p}$, which on using into (4.69), we get

$$\bar{p} = 2\pi i \frac{\omega\rho}{k^4} \int_0^b \phi_1(r, 0) r dr. \tag{4.70}$$

Consequently, the dimensionless impedance Z takes the form

$$Z = \frac{2i}{b^2\nu_0} \int_0^b \phi_1(r, 0) r dr. \tag{4.71}$$

On using (4.4), we get

$$Z = \frac{2i}{b^2\nu_0} \sum_{n=0}^{\infty} (A_n + B_n) \int_0^b R_{1n}(r) r dr, \tag{4.72}$$

or

$$Z = \frac{2i}{b^2\nu_0} \sum_{n=0}^{\infty} A_n Q_m. \tag{4.73}$$

Chapter 5

Conclusion

This chapter summarizes and concludes the present study, highlighting the key findings and contributions of the research. This thesis investigates the reflection and transmission of acoustic waves in cylindrical waveguides with membrane interfaces. And presents a comprehensive investigation of three key areas:

- Micro-perforated panel in cylindrical duct excited by plane piston
- Mathematical modelling of plane piston with elastic membrane
- Scattering of piston radiation from rigid cavity

Chapter 1 provides a solid foundation for the research, introducing the context and background, reviewing relevant literature, and outlining the thesis structure. This chapter summarizes the key findings and contributions of the research, providing a concise overview of the study's outcomes and implications.

Chapter 2 presents fundamental definitions and derivations that are crucial for understanding the mathematical modeling and analysis presented in the subsequent chapters. This chapter provides a solid foundation in the key concepts and mathematical tools used in the research, paving the way for the in-depth exploration of the topic in the chapters that follow.

Chapter 3 introduces a prototype problem to model and solve this physical phenomenon, consisting of the propagation of acoustic waves from a membrane panel in a waveguide radiated by a planar wave. This problem is solved using the mode-matching technique, and the accuracy of the solution is confirmed through

- Reconstruction of the matching condition and

- Satisfaction of the power identity.

The numerical results show the impact of eigenmode trajectories on wave propagation against the velocity of the plane piston.

Chapter 4 examines the propagation of acoustic waves from a membrane panel in a waveguide emitted by a planar piston To tackle this problem, two prototype problems are introduced and solved using the mode-matching technique. The first problem involves mathematical modeling of a plane piston with a micro perforated elastic membrane at the interface, while the second problem involves scattering of piston radiation from a rigid cavity. The accuracy of the solutions is confirmed by reconstructing the matching conditions, which are reformulated using the truncated form of the solution. The satisfaction of these reformulated matching conditions verifies the accuracy of the obtained solutions.

Bibliography

[1] M Åbom. Derivation of four-pole parameters including higher order mode effects for expansion chamber mufflers with extended inlet and outlet. *Journal of Sound and Vibration*, 137(3):403–418, 1990.

[2] M Afzal, T Nawaz, and R Nawaz. Scattering characteristics of planar trifurcated waveguide structure containing multiple discontinuities. *Waves in Random and Complex Media*, 32(6):2776–2795, 2022.

[3] Muhammad Afzal and Hazrat Bilal. Acoustic wave scattering from a wave-bearing cavity in a rectangular waveguide. *The Journal of the Acoustical Society of America*, 144(3_Supplement):1681–1681, 2018.

[4] Muhammad Afzal, Rab Nawaz, Muhammad Ayub, and Abdul Wahab. Acoustic scattering in flexible waveguide involving step discontinuity. *PloS one*, 9(8):e103807, 2014.

[5] Muhammad Afzal, Rab Nawaz, and Aasim Ullah. Attenuation of dissipative device involving coupled wave scattering and change in material properties. *Applied Mathematics and Computation*, 290:154–163, 2016.

[6] Muhammad Afzal, Junaid Uzair Satti, and Rab Nawaz. Scattering characteristics of non-planar trifurcated waveguides. *Meccanica*, 55(5):977–988, 2020.

[7] Muhammad Afzal and Sajid Shafique. Attenuation analysis of flexural modes with absorbent lined flanges and different edge conditions. *The Journal of the Acoustical Society of America*, 148(1):85–99, 2020.

[8] Muhammad Afzal, Sajid Shafique, and Abdul Wahab. Analysis of traveling waveform of flexible waveguides containing absorbent material along flanged

junctions. *Communications in Nonlinear Science and Numerical Simulation*, 97:105737, 2021.

[9] M Ayub, MH Tiwana, and AB Mann. Acoustic diffraction in a trifurcated waveguide with mean flow. *Communications in Nonlinear Science and Numerical Simulation*, 15(12):3939–3949, 2010.

[10] M Ayub, MH Tiwana, and AB Mann. Acoustic diffraction in a trifurcated waveguide with mean flow. *Communications in Nonlinear Science and Numerical Simulation*, 15(12):3939–3949, 2010.

[11] Roger E Behrend, Paul A Pearce, and David L O'Brien. Interaction-round-a-face models with fixed boundary conditions: the abf fusion hierarchy. *Journal of statistical physics*, 84:1–48, 1996.

[12] Abhinav Bhardwaj, Kumar Vaibhav Srivastava, and S A Ramakrishna. Propagation of wave in a cylindrical waveguide filled with hyperbolic negative index medium. *Microwave and Optical Technology Letters*, 62, 06 2020.

[13] Edward J Brambley and Nigel Peake. Classification of aeroacoustically relevant surface modes in cylindrical lined ducts. *Wave motion*, 43(4):301–310, 2006.

[14] Alex DD Craik. "continuity and change": representing mass conservation in fluid mechanics. *Archive for history of exact sciences*, 67:43–80, 2013.

[15] A Cummings and I-J Chang. Sound attenuation of a finite length dissipative flow duct silencer with internal mean flow in the absorbent. *Journal of Sound and Vibration*, 127(1):1–17, 1988.

[16] FD Denia, A Selamet, MJ Martínez, and FJ Fuenmayor. Sound attenuation of a circular multi-chamber hybrid muffler. *Noise control engineering journal*, 56(5):356–364, 2008.

[17] Shota Fujita, Kimihiro Sakagami, Motoki Yairi, Emi Toyoda, and Masayuki Morimoto. An experimental study of a cylindrical microperforated panel sond absorber with core. *Noise Control Engineering Journal*, 61(6), 2013.

[18] Luigi Genovese, Thierry Deutsch, Alexey Neelov, Stefan Goedecker, and Gregory Beylkin. Efficient solution of poisson's equation with free boundary conditions. *The Journal of chemical physics*, 125(7), 2006.

[19] Yuan Gu, Ying Cheng, Jingshi Wang, and Xiaojun Liu. Controlling sound transmission with density-near-zero acoustic membrane network. *Journal of Applied Physics*, 118(2), 2015.

[20] Lixi Huang. Modal analysis of a drumlike silencer. *the Journal of the Acoustical Society of America*, 112(5):2014–2025, 2002.

[21] Rahmatullah Ibrahim Nuruddeen, Rab Nawaz, and QM Zaigham Zia. Asymptotic approach to anti-plane dynamic problem of asymmetric three-layered composite plate. *Mathematical Methods in the Applied Sciences*, 44(14):10933–10947, 2021.

[22] Uno Ingård. On the radiation of sound into a circular tube, with an application to resonators. *The Journal of the Acoustical Society of America*, 20(5):665–682, 1948.

[23] J Kang and HV Fuchs. Predicting the absorption of open weave textiles and micro-perforated membranes backed by an air space. *Journal of sound and vibration*, 220(5):905–920, 1999.

[24] Woojin Kim and Haecheon Choi. Immersed boundary methods for fluid-structure interaction: A review. *International Journal of Heat and Fluid Flow*, 75:301–309, 2019.

[25] Ray Kirby, Paul Williams, and James Hill. A comparison between the performance of different silencer designs for gas turbine exhaust systems. In *Acoustics 2012*, 2012.

[26] Jane B Lawrie. On eigenfunction expansions associated with wave propagation along ducts with wave-bearing boundaries. *IMA journal of applied mathematics*, 72(3):376–394, 2007.

[27] Jane B Lawrie. Comments on a class of orthogonality relations relevant to fluid-structure interaction. *Journal of Engineering Mathematics*, 2012.

[28] Jane B Lawrie and I David Abrahams. An orthogonality relation for a class of problems with high-order boundary conditions; applications in sound-structure interaction. *The Quarterly Journal of Mechanics and Applied Mathematics*, 52(2):161–181, 1999.

[29] Jane B Lawrie and Muhammad Afzal. Acoustic scattering in a waveguide with a height discontinuity bridged by a membrane: a tailored galerkin approach. *Journal of Engineering Mathematics*, 105:99–115, 2017.

[30] Harold Levine and Julian Schwinger. On the radiation of sound from an unflanged circular pipe. *Physical review*, 73(4):383, 1948.

[31] Chenxi Li, Ben Cazzolato, and Anthony Zander. Acoustic impedance of micro perforated membranes: Velocity continuity condition at the perforation boundary. *The Journal of the Acoustical Society of America*, 139(1):93–103, 2016.

[32] Nathan Marcuvitz. *Waveguide handbook*. Number 21. Iet, 1951.

[33] K Mazaheri and PL Roe. Numerical wave propagation and steady-state solutions: Soft wall and outer boundary conditions. *AIAA journal*, 35(6):965–975, 1997.

[34] John W Miles. The analysis of plane discontinuities in cylindrical tubes. part i. *The Journal of the Acoustical Society of America*, 17(3):259–271, 1946.

[35] Jianwei Mu and Wei-Ping Huang. Simulation of three-dimensional waveguide discontinuities by a full-vector mode-matching method based on finite-difference schemes. *Optics express*, 16(22):18152–18163, 2008.

[36] R Nawaz, Rahmatullah Ibrahim Nuruddeen, and QM Zaigham Zia. An asymptotic investigation of the dynamics and dispersion of an elastic five-layered plate for anti-plane shear vibration. *Journal of Engineering Mathematics*, 128(1):9, 2021.

[37] Rab Nawaz, Muhammad Afzal, and Muhammad Ayub. Acoustic propagation in two-dimensional waveguide for membrane bounded ducts. *Communications in Nonlinear Science and Numerical Simulation*, 20(2):421–433, 2015.

[38] Rab Nawaz, Aasim Ullah Jan, and Muhammad Afzal. Fluid-structure coupled wave scattering in a flexible duct at the junction of planar discontinuities. *Advances in Mechanical Engineering*, 9(7):1687814017713187, 2017.

[39] Rab Nawaz and Jane B Lawrie. Scattering of a fluid-structure coupled wave at a flanged junction between two flexible waveguides. *The Journal of the Acoustical Society of America*, 134(3):1939–1949, 2013.

[40] Touqeer Nawaz, Muhammad Afzal, and Rab Nawaz. The scattering analysis of trifurcated waveguide involving structural discontinuities. *Advances in Mechanical Engineering*, 11(7):1687814019829282, 2019.

[41] Touqeer Nawaz, Muhammad Afzal, and Abdul Wahab. Scattering analysis of a flexible trifurcated lined waveguide structure with step-discontinuities. *Physica Scripta*, 96(11):115004, 2021.

[42] Rahmatullah Ibrahim Nuruddeen, R Nawaz, and QM Zaigham Zia. Asymptotic analysis of an anti-plane shear dispersion of an elastic five-layered structure amidst contrasting properties. *Archive of Applied Mechanics*, 90:1875–1892, 2020.

[43] Rahmatullah Ibrahim Nuruddeen, R Nawaz, and QM Zaigham Zia. Investigating the viscous damping effects on the propagation of rayleigh waves in a three-layered inhomogeneous plate. *Physica Scripta*, 95(6):065224, 2020.

[44] Rahmatullah Ibrahim Nuruddeen, Rab Nawaz, and Qazi Muhammad Zaigham Zia. Effects of thermal stress, magnetic field and rotation on the dispersion of elastic waves in an inhomogeneous five-layered plate with alternating components. *Science Progress*, 103(3):0036850420940469, 2020.

[45] Rahmatullah Ibrahim Nuruddeen, Rab Nawaz, and Qazi Muhammad Zia. Dispersion of elastic waves in an asymmetric three-layered structure in the presence of magnetic and rotational effects. *Progress In Electromagnetics Research M*, 91:165–177, 2020.

[46] Kazuhiko Ogusu. Numerical analysis of the rectangular dielectric waveguide and its modifications. *IEEE Transactions on microwave theory and techniques*, 25(11):874–885, 1977.

[47] Lili Pan and Francesco Martellotta. A parametric study of the acoustic performance of resonant absorbers made of micro-perforated membranes and perforated panels. *Applied Sciences*, 10(5):1581, 2020.

[48] AD Rawlins et al. Sound radiation in a planar trifurcated lined duct. *Wave Motion*, 29(2):157–174, 1999.

[49] Sjoerd W Rienstra. A classification of duct modes based on surface waves. *Wave motion*, 37(2):119–135, 2003.

[50] Junaid Uzair Satti, Muhammad Afzal, and Rab Nawaz. Scattering analysis of a partitioned wave-bearing cavity containing different material properties. *Physica Scripta*, 94(11):115223, 2019.

[51] Jan Schorer and Jens Bornemann. A mode-matching technique for the analysis of waveguide-on-substrate components. In *2015 IEEE MTT-S International Conference on Numerical Electromagnetic and Multiphysics Modeling and Optimization (NEMO)*, pages 1–3, 2015.

[52] A Selamet, MB Xu, I-J Lee, and NT Huff. Analytical approach for sound attenuation in perforated dissipative silencers. *The Journal of the Acoustical Society of America*, 115(5):2091–2099, 2004.

[53] Sajid Shafique, Muhammad Afzal, and Rab Nawaz. On the attenuation of fluid–structure coupled modes in a non-planar waveguide. *Mathematics and Mechanics of Solids*, 25(10):1831–1850, 2020.

[54] EL Shenderov. Helmholtz equation solutions corresponding to multiple roots of the dispersion equation for a waveguide with impedance walls. *Acoustical physics*, 46(3):357–363, 2000.

[55] William A Sirignano. Compressible flow at high pressure with linear equation of state. *Journal of Fluid Mechanics*, 843:244–292, 2018.

[56] George Gabriel Stokes. On the theories of the internal friction of fluids in motion, and of the equilibrium and motion of elastic solids. *Fluids*, 2007.

[57] C Sujatha. Fundamentals of acoustics. In *Vibration, Acoustics and Strain Measurement: Theory and Experiments*, pages 161–217. Springer, 2023.

[58] Mahmood ul Hassan. Wave scattering by soft-hard three spaced waveguide. *Applied Mathematical Modelling*, 38(17-18):4528–4537, 2014.

[59] JAM Van Ostaay, AR Akhmerov, CWJ Beenakker, and M Wimmer. Dirac boundary condition at the reconstructed zigzag edge of graphene. *Physical Review B—Condensed Matter and Materials Physics*, 84(19):195434, 2011.

[60] Xu Wang and Cheuk-Ming Mak. Wave propagation in a duct with a periodic helmholtz resonators array. *The Journal of the Acoustical Society of America*, 131(2):1172–1182, 2012.

[61] Zhanjiang Wang, Hao Yu, and Qian Wang. Layer-substrate system with an imperfectly bonded interface: spring-like condition. *International Journal of Mechanical Sciences*, 134:315–335, 2017.

[62] MB Xu, A Selamet, I-J Lee, and NT Huff. Sound attenuation in dissipative expansion chambers. *Journal of Sound and Vibration*, 272(3-5):1125–1133, 2004.